Brazilian Journal of Physics (2018) 48:190–213
https://doi.org/10.1007/s13538-017-0552-6

GENERAL AND APPLIED PHYSICS

Review of Progress in Acoustic Levitation

Marco A. B. Andrade[1] · Nicolás Pérez[2] · Julio C. Adamowski[3]

Received: 31 October 2017 / Published online: 30 December 2017

Abstract
Acoustic levitation uses acoustic radiation forces to counteract gravity and suspend objects in mid-air. Although acoustic levitation was first demonstrated almost a century ago, for a long time, it was limited to objects much smaller than the acoustic wavelength levitating at fixed positions in space. Recent advances in acoustic levitation now allow not only suspending but also rotating and translating objects in three dimensions. Acoustic levitation is also no longer restricted to small objects and can now be employed to levitate objects larger than the acoustic wavelength. This article reviews the progress of acoustic levitation, focusing on the working mechanism of different types of acoustic levitation devices developed to date. We start with a brief review of the theory. Then, we review the acoustic levitation methods to suspend objects at fixed positions, followed by the techniques that allow the manipulation of objects. Finally, we present a brief summary and offer some future perspectives for acoustic levitation.

Keywords Acoustics · Acoustic levitation · Acoustic radiation force

1 Introduction

Wingardium Leviosa! When pronouncing these words, in combination with the swish and flick of a wand, characters from the movie Harry Potter can levitate objects [1]. In contrast, scientists do not need a magic wand, since we can use a variety of noncontact forces to counteract gravity and truly suspend objects in mid-air. Distinct techniques are available to levitate objects, including magnetic, electric, optical, aerodynamic, and acoustic levitation (a comprehensive review of these methods is provided by Brandt [2]). In this review, we focus on the acoustic levitation method, mainly because it has the ability to levitate almost any kind of material, including solids [3–5], liquids [6–8], and even small living animals [9, 10]. This versatility makes acoustic levitation a promising tool in analytical chemistry [11, 12], material sciences [13], pharmacy [14], microassembly [15], etc.

✉ Marco A. B. Andrade
marcobrizzotti@gmail.com

[1] Institute of Physics, University of São Paulo, São Paulo 05508-090, Brazil

[2] Facultad de Ingeniería, Universidad de La República, 11200 Montevideo, Uruguay

[3] Escola Politécnica, University of São Paulo, São Paulo 05508-030, Brazil

For many years, acoustic levitation has been used mainly to suspend small objects at fixed positions in space, but in recent years, significant progress has been made and there are now numerous acoustic levitation strategies to manipulate the levitated object in mid-air. The physical principle behind acoustic levitation has been even extended to liquid media, where it has been used to trap and to manipulate microparticles and cells in a water medium (see review papers [16–19] for "levitation" in liquids).

This article reviews the acoustic levitation methods developed to levitate and to manipulate objects in mid-air. Our focus is to explain the working principle of different types of acoustic levitation devices. The potential applications of acoustic levitation in the areas of analytical chemistry [11, 12], biophysics [20], and microassembly [15] have been reviewed elsewhere and will not be covered here. We start this article by presenting the theory behind acoustic levitation. In Section 3, the acoustic levitation methods capable of levitating objects at fixed positions in space are reviewed. The levitation methods capable of manipulating the levitated objects are presented in Section 4. We conclude with a summary and discuss future possibilities of acoustic levitation.

2 Theory

In this section, we present an overview of the theory behind the acoustic levitation of objects in an ideal fluid. As we shall

see, acoustic levitation uses acoustic radiation pressure to counteract gravity and suspend matter in air. Acoustic radiation pressure has been studied by a number of researchers [21–26], and an in-depth coverage of this subject is beyond the scope of this review. For now, we would like to emphasize that although we can easily apply the expressions for the acoustic radiation pressure to calculate the radiation force on objects, the physics behind the radiation pressure is not so simple as it first appears. This difficulty is nicely illustrated by what Beyer once wrote: "It might be said that radiation pressure is a phenomenon that the observer thinks he understands—for short intervals, and only every now and then." [27]. Therefore, it is not our intent to discuss all the physics behind the radiation pressure and the interested reader can refer to review articles [27–31] and tutorial papers [32–34] for further details.

We start this section by presenting the governing equations of fluid motion, followed by a derivation of the linear wave equation. The governing equations are then combined to obtain the acoustic radiation pressure, and a simple analytical expression for the acoustic radiation force acting on a small sphere is presented. This expression is used to obtain the radiation force acting on a small rigid sphere in a plane acoustic standing wave field. In addition, a numerical procedure to obtain the acoustic radiation force on levitating objects is presented. To simplify the analysis, we assume an inviscid fluid and nonlinear effects such as acoustic streaming [35–37] and harmonic generation [38] are not considered. We also neglect the acoustic interaction forces [39, 40] caused by the wave scattering from other objects.

2.1 Governing Equations of Fluid Motion

The motion of a fluid element of infinitesimal volume (dV), containing a large number of molecules, such that it can be considered as a continuous medium, can be described in terms of its velocity vector ($\mathbf{u}$), density (ρ), and pressure (p). These fields can vary in space and time and are consequently functions of position ($\mathbf{r}$) and time (t). To describe the fluid motion, we adopt a Cartesian coordinate system in which the position vector $\mathbf{r} = x\hat{\mathbf{i}} + y\hat{\mathbf{j}} + z\hat{\mathbf{k}}$ is written in terms of the Cartesian unit vectors $\hat{\mathbf{i}}$, $\hat{\mathbf{j}}$, and $\hat{\mathbf{k}}$. To simplify the analysis, we assume that the fluid is inviscid and nonheat-conductive. In this case, three equations are required to describe the fluid motion: equation of continuity, equation of conservation of momentum, and equation of state of the fluid. Deriving these equations is beyond the scope of this paper, and the detailed derivation and discussion can be found in numerous textbooks [41–43]. The first equation, related with the conservation of mass, is the equation of continuity, given by

$$\frac{\partial \rho}{\partial t} + \nabla\cdot(\rho\mathbf{u}) = 0. \tag{1}$$

The second equation is the equation of conservation of momentum. Neglecting the gravitational field and considering an inviscid fluid, the equation of conservation of momentum can be expressed by

$$\rho\left[\frac{\partial \mathbf{u}}{\partial t} + (\mathbf{u}\cdot\nabla)\mathbf{u}\right] = -\nabla p. \tag{2}$$

This equation is also called Euler's equation. Finally, we also need the equation of state of the fluid that relates the fluid density with the pressure. The equation of state of the fluid provides a macroscopic description of the interaction between the molecules of a fluid. In the simplest case of a rarefied gas at high temperatures, the interaction forces between molecules can be neglected and the gas can be described by the ideal gas law. However, when the pressure increases, the equation of state of the fluid becomes more complex and can be described by

$$p = p(\rho) \tag{3}$$

which expresses the pressure in terms of the fluid density.

2.2 Linear Wave Equation

The set of Eqs. (1)–(3) can be combined to describe the propagation of mechanical waves in fluids. However, these equations are nonlinear and finding an analytical solution to these equations is not an easy task, even in the simplest cases. Fortunately, we can simplify Eqs. (1)–(3) by assuming that the mechanical waves have small amplitudes.

To describe the propagation of mechanical waves of small amplitudes in a fluid medium, let us consider that in the absence of the wave, the fluid is at rest ($\mathbf{u} = 0$) and has constant pressure (p_0) and constant density (ρ_0). Let us also assume that when a wave propagates in the fluid, the fields p, $\mathbf{u}$, and ρ present small variations in relation to the unperturbed fluid. In this case, we can express the total fields (p, $\mathbf{u}$, and ρ) as a sum of the unperturbed fields (p_0, $\mathbf{u}_0$, and ρ_0) and the first-order perturbation fields (p_1, $\mathbf{u}_1$, and ρ_1), as follows:

$$p = p_0 + p_1, \tag{4a}$$

$$\mathbf{u} = \mathbf{u}_0 + \mathbf{u}_1 = \mathbf{u}_1, \tag{4b}$$

$$\rho = \rho_0 + \rho_1. \tag{4c}$$

In Eqs. (4a)–(4c), subscript 0 refers to the unperturbed fields and subscript 1 is used for the first-order approximations. Here, the unperturbed fluid is assumed to be at rest, such that the unperturbed velocity ($\mathbf{u}_0$) is equal to zero. In addition, when dealing with waves of small amplitudes, we can also consider that $|p_1| << p_0$ and $|\rho_1| << \rho_0$. By using these approximations and replacing Eqs. (4b) and (4c) in Eq. (1), we obtain the linearized continuity equation

$$\frac{\partial \rho_1}{\partial t} + \nabla\cdot(\rho_0 \mathbf{u}_1) = 0. \tag{5}$$

Similarly, the linearized momentum equation can be obtained by assuming that $|(\mathbf{u}\cdot\nabla)\mathbf{u}| << |\partial\mathbf{u}/\partial t|$. Therefore, replacing Eqs. (4a)–(4c) in Eq. (2) and neglecting the term $(\mathbf{u}\cdot\nabla)\mathbf{u}$, we obtain

$$\rho_0 \frac{\partial \mathbf{u}_1}{\partial t} = -\nabla p_1 \tag{6}$$

which is the linearized momentum equation for an ideal fluid. This equation is also called the linear Euler's equation. Finally, the linear form of the equation of state of the fluid can be obtained by expanding Eq. (3) in Taylor's series

$$p = p_0 + \left(\frac{\partial p}{\partial \rho}\right)_{\rho_0} (\rho - \rho_0) + \ldots. \tag{7}$$

By rearranging the terms of Eq. (7), we obtain

$$p - p_0 = \rho_0 \left(\frac{\partial p}{\partial \rho}\right)_{\rho_0} \frac{(\rho - \rho_0)}{\rho_0} \tag{8}$$

which can be expressed by

$$p_1 = \rho_0 \left(\frac{\partial p}{\partial \rho}\right)_{\rho_0} \frac{\rho_1}{\rho_0} = \frac{B}{\rho_0}\rho_1 \tag{9}$$

where

$$B = \rho_0 \left(\frac{\partial p}{\partial \rho}\right)_{\rho_0} \tag{10}$$

is the adiabatic bulk modulus of the fluid. In Eq. (9), we can also replace B/ρ_0 by c_0^2, where c_0 is the isentropic speed of sound in the fluid. Therefore, we can finally write the equation of state of the fluid in the linearized form as

$$p_1 = c_0^2 \rho_1. \tag{11}$$

The linearized Eqs. (5), (6), and (11) can be combined to obtain the linear wave equation. First, we replace Eq. (11) in Eq. (5) and then derive the resulting equation in respect to t, resulting in

$$\frac{1}{c_0^2}\frac{\partial^2 p_1}{\partial t^2} + \nabla\cdot\left(\rho_0 \frac{\partial \mathbf{u}_1}{\partial t}\right) = 0. \tag{12}$$

Finally, replacing Eq. (6) in Eq. (12), yields

$$\nabla^2 p_1 = \frac{1}{c_0^2}\frac{\partial^2 p_1}{\partial t^2}, \tag{13}$$

which is the linear wave equation. From this equation, it becomes evident that c_0, introduced earlier, corresponds to the speed of sound in the fluid medium. Equation (13) can be solved to obtain the acoustic pressure (p_1) in space as a function of time. From the acoustic pressure (p_1), the velocity field ($\mathbf{u}_1$) and the density field (ρ_1) can be easily found by using Eqs. (6) and (11), respectively.

It is also worth mentioning that the particle velocity ($\mathbf{u}_1$), associated with a sound wave in an inviscid fluid, is irrotational, which means it can be expressed as a gradient of a scalar function (ϕ_1)

$$\mathbf{u}_1 = \nabla\phi_1. \tag{14}$$

The scalar function (ϕ_1) is called the velocity potential, and it can be demonstrated [42] that it is also a solution of the wave equation, given by

$$\nabla^2\phi_1 = \frac{1}{c_0^2}\frac{\partial^2\phi_1}{\partial t^2}. \tag{15}$$

In many situations, it is useful to solve Eq. (15) to find the velocity potential and then calculate the acoustic pressure and the velocity fields from the velocity potential. Knowing the potential ϕ_1, the velocity field ($\mathbf{u}_1$) can be calculated by using Eq. (14) and the acoustic pressure (p_1) can be determined by replacing Eq. (14) into Eq. (6), resulting in

$$p_1 = -\rho_0 \frac{\partial\phi_1}{\partial t}. \tag{16}$$

Many acoustic problems involve the propagation of time-harmonic fields. The mathematical treatment of time-harmonic acoustic waves can be simplified by adopting complex numbers. In this case, the velocity potential can be described by

$$\phi_1(\mathbf{r}, t) = \phi_1(\mathbf{r})\mathrm{e}^{-i\omega t}. \tag{17}$$

where i is the imaginary unit and $\omega = 2\pi f$ is the angular frequency, with f being the frequency. The advantage of adopting complex numbers is that we can easily obtain the amplitudes and phases of the fields p_1, $\mathbf{u}_1$, and ρ_1 by taking the moduli and the arguments of the corresponding complex fields. In addition, the real physical solution can be easily determined by taking the real part of the complex fields.

Replacing Eq. (17) in Eq. (15) yields the time-independent form of the wave equation, expressed as

$$\nabla^2\phi_1 + k^2\phi_1 = 0. \tag{18}$$

This is the Helmholtz equation, where $k = z/c_0 = 2\pi/\lambda$ is the wavenumber and λ is the wavelength.

2.3 Acoustic Radiation Pressure

Many acoustical problems can be accurately described by the linear wave equation. However, the first-order approximation described in Section 2.2 is not capable of predicting an

important nonlinear phenomenon in acoustics: the acoustic radiation pressure [27]. In order to describe the radiation pressure, we must include second-order effects in our analysis. In the second-order approximation, the fields p, $\mathbf{u}$, and ρ are described by

$$p = p_0 + p_1 + p_2 \tag{19a}$$

$$\mathbf{u} = \mathbf{u}_1 + \mathbf{u}_2 \tag{19b}$$

$$\rho = \rho_0 + \rho_1 + \rho_2. \tag{19c}$$

Replacing Eqs. (19a)–(19c) in Eq. (2) and keeping only the second order terms, we obtain

$$\nabla p_2 = -\rho_0 \frac{\partial \mathbf{u}_2}{\partial t} - \rho_1 \frac{\partial \mathbf{u}_1}{\partial t} - \rho_0 (\mathbf{u}_1 \cdot \nabla)\mathbf{u}_1. \tag{20}$$

Although p_2 varies with time, most applications involving acoustic radiation pressure use high-frequency time-harmonic fields, whose observable effects occur in a much slower time scale. Consequently, we can simplify the mathematical treatment by calculating the time-averaged value of p_2 over a large number of cycles. Therefore, by time-averaging Eq. (20), we find

$$\nabla \langle p_2 \rangle = -\rho_0 \left\langle \frac{\partial \mathbf{u}_2}{\partial t} \right\rangle - \left\langle \rho_1 \frac{\partial \mathbf{u}_1}{\partial t} \right\rangle - \rho_0 \langle (\mathbf{u}_1 \cdot \nabla)\mathbf{u}_1 \rangle, \tag{21}$$

where the angle brackets $\langle\rangle$ represent the time average. As discussed by Bruus [44], the second-order velocity ($\mathbf{u}_2$) is periodic for a time-harmonic field, and its decomposition in Fourier series results in a sum of sinusoidal waves and a constant. The time average of these sinusoidal waves and the time derivative of the constant are both zero. Therefore, the first term on the right-hand side of Eq. (21) is also zero, resulting in

$$\nabla \langle p_2 \rangle = -\left\langle \rho_1 \frac{\partial \mathbf{u}_1}{\partial t} \right\rangle - \rho_0 \langle (\mathbf{u}_1 \cdot \nabla)\mathbf{u}_1 \rangle. \tag{22}$$

Finally, by combining Eqs. (6), (11), and (22) and using $\nabla \left(p_1^2\right) = 2p_1 \nabla p_1$ and $\nabla(\mathbf{u_1} \cdot \mathbf{u_1}) = 2(\mathbf{u}_1 \cdot \nabla)\mathbf{u}_1$, we obtain

$$\langle p_2 \rangle = \frac{1}{2\rho_0 c_0^2} \langle p_1^2 \rangle - \frac{\rho_0}{2} \langle \mathbf{u}_1 \cdot \mathbf{u}_1 \rangle \tag{23}$$

which is the time-averaged acoustic radiation pressure. Although the radiation pressure $\langle p_2 \rangle$ is a nonlinear phenomenon, it can be calculated from the linear fields p_1 and $\mathbf{u}_1$. From the acoustic radiation pressure, given by Eq. (23), the acoustic radiation force ($\mathbf{F_{rad}}$) acting on a rigid object of arbitrary shape and size is calculated by

$$\mathbf{F_{rad}} = -\int_{S_0} \langle p_2 \rangle \mathbf{n} dS. \tag{24}$$

The problem of determining the acoustic radiation force on a rigid object is illustrated in Fig. 1a. In this figure, an incident acoustic field represented by the acoustic pressure (p_1^{in}) and the particle velocity ($\mathbf{u}_1^{in}$) is scattered by the object. The scattered wave is represented by the fields p_1^{sc} and $\mathbf{u}_1^{sc}$. The superposition of the incident and scattered waves results in the total fields $p_1 = p_1^{in} + p_1^{sc}$ and $\mathbf{u}_1 = \mathbf{u}_1^{in} + \mathbf{u}_1^{sc}$. From the total fields, the time-averaged acoustic radiation pressure is calculated by Eq. (23) and the acoustic radiation force that acts on the object is obtained from Eq. (24). In Eq. (24), $\mathbf{n}$ represents the surface normal vector and the integral is evaluated over the surface of the object, represented by S_0 in Fig. 1a.

Equation (24) is useful to obtain the acoustic radiation force acting on a rigid object in a fixed position in space [45, 46]. However, for compressible objects, the object surface can move in the presence of an acoustic field. In this case, the acoustic radiation force ($\mathbf{F_{rad}}$) acting on the object can be determined by [24, 34]

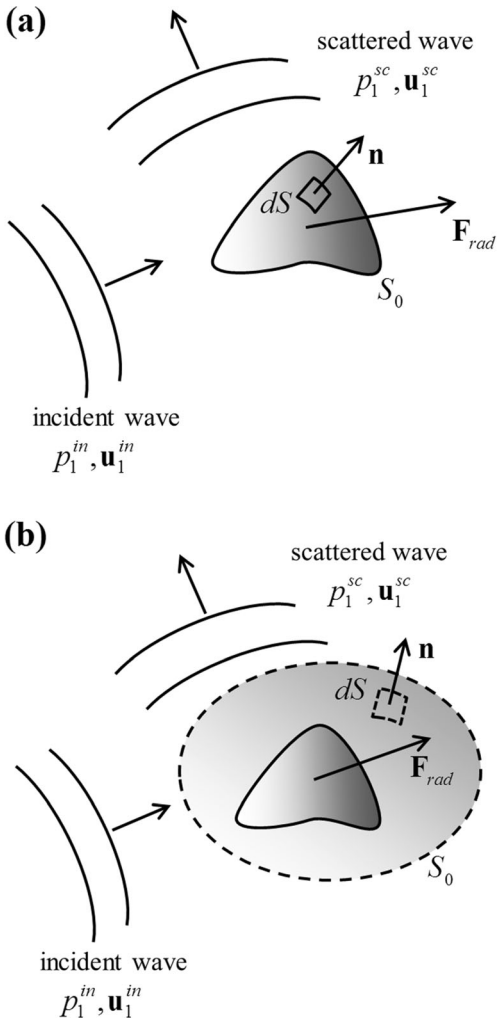

Fig. 1 Two approaches to calculate the acoustic radiation force ($\mathbf{F_{rad}}$) acting on an object in an acoustic field. In the first approach, illustrated in **a**, the radiation pressure is integrated over the object surface, while in **b**, the integration is performed in a closed surface S_0 encompassing the object. In **a**, the acoustic radiation force is calculated through Eq. (24), and in **b**, the radiation force is given by Eq. (25)

$$\mathbf{F_{rad}} = -\int_{S_0}\langle p_2\rangle \mathbf{n} dS - \int_{S_0}\rho_0\langle(\mathbf{n}\cdot\mathbf{u}_1)\mathbf{u}_1\rangle dS. \quad (25)$$

In Eq. (25), the integral is evaluated in a closed surface S_0 encompassing the object. This approach of determining the acoustic radiation force on an object is illustrated in Fig. 1b. This second approach is particularly useful for computing the radiation force on compressible objects immersed in a liquid medium. For most solid objects in air, there is a significant difference between the air density and the object density, such that the object can be considered as a rigid material. In this case, both approaches can be applied to obtain $\mathbf{F_{rad}}$.

2.4 Acoustic Radiation Force on a Small Sphere in an Arbitrary Acoustic Field

A very useful expression to obtain the acoustic radiation force that acts on a small sphere in an arbitrary acoustic field was derived by Gor'kov [25]. The original paper in Russian and its translation to English [25] is very succinct, and the step-by-step derivation of the Gor'kov expression can be found elsewhere [34, 47]. In his derivation, Gor'kov assumed that a sphere of radius (R) much smaller than the acoustic wavelength (λ) is immersed in an acoustic field in an ideal fluid. The radiation force ($\mathbf{F_{rad}}$) acting on the small sphere is expressed in terms of the potential of the acoustic radiation force (U), given by [25]

$$U = 2\pi R^3\left[\frac{f_1}{3\rho_0 c_0^2}\left\langle\left(p_1^{in}\right)^2\right\rangle - \frac{f_2\rho_0}{2}\left\langle\mathbf{u}_1^{in}\cdot\mathbf{u}_1^{in}\right\rangle\right] \quad (26)$$

where p_1^{in} and $\mathbf{u}_1^{in}$ are, respectively, the first-order incident acoustic pressure and particle velocity at the sphere position. Equation (26) is the famous Gor'kov expression, which has been widely used to obtain the radiation force acting on levitating particles in air [4, 48–53] as well as in microparticles in liquid media [17, 19]. Factors f_1 and f_2 depend on the mechanical properties of the sphere and the fluid medium and are calculated through the expressions

$$f_1 = 1 - \frac{\rho_0 c_0^2}{\rho_p c_p^2} \quad (27)$$

$$f_2 = 2\left(\frac{\rho_p - \rho_0}{2\rho_p + \rho_0}\right). \quad (28)$$

In Eqs. (27) and (28), ρ_p and c_p are the sphere density and speed of sound in the sphere, respectively. In most acoustic levitation experiments in air, we can assume that the sphere density is much larger than the air density, leading to $f_1 = f_2 = 1$. From the potential (U) (also called the Gor'kov potential), the acoustic radiation force on the small sphere is calculated through

$$\mathbf{F_{rad}} = -\nabla U. \quad (29)$$

The main advantage of using the Gor'kov expression is that the acoustic radiation force is entirely calculated by considering only the incident fields p_1^{in} and $\mathbf{u}_1^{in}$ at the position of the sphere.

2.5 Acoustic Radiation Force on a Small Rigid Sphere in a Plane Standing Wave Field

In this section, we apply the Gor'kov expression to obtain the acoustic radiation force on a small rigid sphere in a plane standing wave field. As we shall see in Section 3.1, a typical configuration of an acoustic levitation device consists of an ultrasonic transducer and a reflecting surface in which an acoustic standing wave field is established between them. Due to the action of the acoustic radiation force, a small object can be levitated around the pressure nodes of the standing wave. In order to calculate the acoustic radiation force that acts on a small rigid sphere, we simplify the problem by assuming a plane standing wave field between the transducer and the reflecting surface, as illustrated in Fig. 2. Although this assumption is not realistic in most levitation devices, it allows deriving a simple analytical expression for the acoustic radiation force that acts on the levitated object.

In order to apply the Gor'kov expression to calculate the acoustic radiation force on a rigid spherical particle of radius $R << \lambda$, we must find the first-order acoustic pressure and the particle velocity distributions between the transducer and the reflector. In an acoustic standing wave, the incident first-order acoustic pressure (p_1^{in}) can be described by

$$p_1^{in} = p_0\cos(\omega t)\cos(kz) \quad (30)$$

where p_0 is the acoustic pressure amplitude. The acoustic pressure (p_1^{in}) given by Eq. (30) is the solution of the linear wave Eq. (13), with $k = \omega/c_0$. By replacing Eq. (30) in Eq. (6), we find the particle velocity ($\mathbf{u_1^{in}}$)

$$\mathbf{u_1^{in}} = \frac{p_0}{\rho_0 c_0}\sin(\omega t)\sin(kz)\hat{\mathbf{k}}. \quad (31)$$

From the first-order fields p_1^{in} and $\mathbf{u_1^{in}}$, given by Eqs. (30) and (31), respectively, we can take the following time averages:

$$\left\langle\left(p_1^{in}\right)^2\right\rangle = \frac{1}{T}\int_t^{t+T} p_0^2\cos^2(\omega t)\cos^2(kz)dt = \frac{p_0^2}{2}\cos^2(kz) \quad (32)$$

$$\left\langle\mathbf{u_1^{in}}\cdot\mathbf{u_1^{in}}\right\rangle = \frac{1}{T}\int_t^{t+T}\left(\frac{p_0}{\rho_0 c_0}\right)^2\sin^2(\omega t)\sin^2(kz)dt = \frac{1}{2}\left(\frac{p_0}{\rho_0 c_0}\right)^2\sin^2(kz). \quad (33)$$

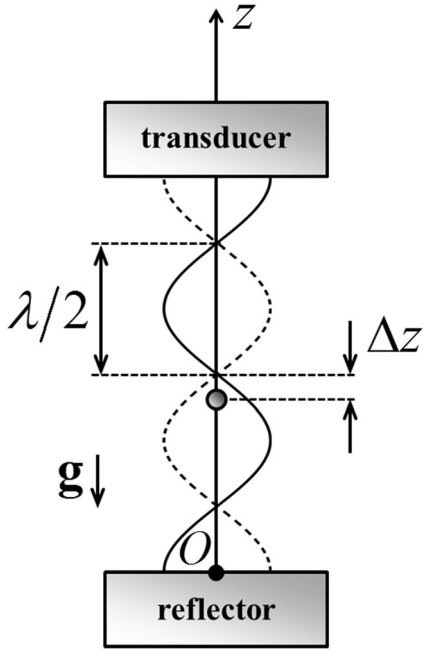

Fig. 2 Acoustic levitation of a small rigid sphere at the pressure node of a plane standing wave established between a transducer and a reflector

By replacing Eqs. (32) and (33) in Eq. (26) and considering $f_1 = f_2 = 1$, we obtain the potential of the acoustic radiation force on a small rigid sphere of radius R, given by

$$U = \frac{p_0^2 \pi R^3}{\rho_0 c_0^2}\left[\frac{\cos^2(kz)}{3} - \frac{\sin^2(kz)}{2}\right]. \tag{34}$$

Finally, the acoustic radiation force on the sphere is

$$\mathbf{F_{rad}} = \frac{5\pi R^3 k p_0^2}{6\rho_0 c_0^2}\sin(2kz)\hat{\mathbf{k}}. \tag{35}$$

The radiation force given by Eq. (35) is identical to that obtained by King in 1934 [23]. Equations (34) and (35) show that the acoustic radiation force that acts on a small rigid sphere in an acoustic standing wave field points towards the pressure nodes of the standing wave field. Figure 3 shows the comparison between the incident acoustic pressure, particle velocity, potential (U), and the radiation force ($\mathbf{F_{rad}}$). In the absence of gravity, the sphere should levitate at the positions where the acoustic pressure is zero, i.e., at $z_n = (n\lambda/2 + \lambda/4)$, with $n = 0, 1, 2,\ldots$. However, due to the action of the gravity acceleration ($\mathbf{g}$), the equilibrium is reached when the object levitates slightly below the acoustic pressure node, at a distance Δz from the node (see Fig. 2).

In the presence of gravity, the small sphere experiences not only the radiation force but also a gravity force ($\mathbf{F_g}$) given by

$$\mathbf{F_g} = -mg\hat{\mathbf{k}} \tag{36}$$

where g is the acceleration of gravity and m is the sphere mass. Now, we can combine Eqs. (35) and (36) to find the minimum

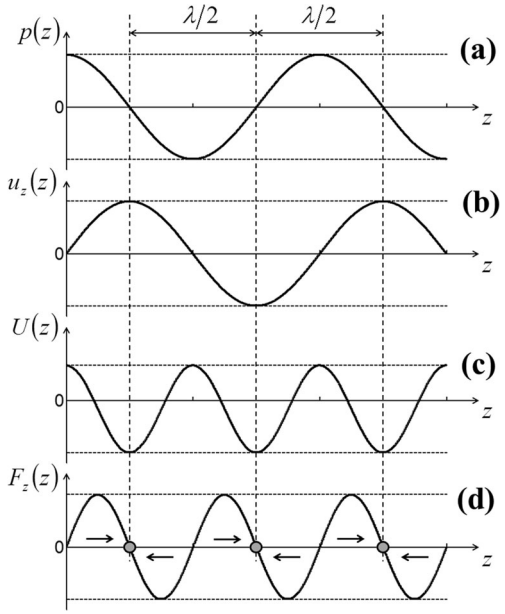

Fig. 3 Acoustic pressure and particle velocity distributions of a plane standing wave and its corresponding potential and radiation force on a small sphere. **a** First-order acoustic pressure. **b** Particle velocity in the z direction. **c** Potential of the radiation force. **d** Acoustic radiation force that acts on the sphere. (Reproduced with permission from [54])

required acoustic pressure amplitude ($p_0^{\min}$) to levitate the sphere. By considering that levitation is possible when the maximum value of $\mathbf{F_{rad}}$ is higher than the gravity force, we obtain

$$p_0^{\min} = \sqrt{\frac{6\rho_0 c_0^2 mg}{5\pi R^3 k}} = \sqrt{\frac{8\rho_0 \rho_p c_0^2 g}{5k}} \tag{37}$$

which is the minimum acoustic pressure amplitude required to levitate a sphere of density (ρ_p). Note that both the gravitational force and the radiation force scale with R^3 and, consequently, the minimum acoustic pressure are independent of the sphere radius (provided that the sphere radius is much smaller than the acoustic wavelength).

Considering a hypothetical standing wave acoustic levitator operating at a frequency of 20 kHz in air ($c_0 =$ 343 m/s and $\rho_0 = 1.2$ kg/m^3), the minimum acoustic pressure amplitude required to levitate a small sphere of density $\rho_p =$ 1000 kg/m^3 in the Earth's environment ($g = 9.8$ m/s^2) is, according to Eq. (37), $p_0^{\min} \approx 2460$ Pa.

In the neighborhood of a pressure node, the acoustic radiation force acting on the levitated object is proportional to its displacement from the node. In this case, the acoustic radiation force can be approximated by the restoring force of a spring [52]. Therefore, for small displacements from the pressure nodes, the radiation force can be described by

$$\mathbf{F_{rad}} = -K(z - z_n)\hat{\mathbf{k}} \tag{38}$$

where z is the sphere vertical position, z_n is the position of the nth pressure node, and K is the elastic constant, given by

$$K = \frac{d^2U}{dz^2} = \frac{5\pi R^3 k^2 p_0^2}{3\rho_0 c_0^2}. \quad (39)$$

This result shows that the radiation force acting on a sphere in the neighborhood of a pressure node can be treated as a fictitious spring where the elastic constant (K) is proportional to the square of the acoustic pressure amplitude. Therefore, differently from a real spring where the elastic constant cannot be altered, we can control the elastic constant of our fictitious acoustic spring just by changing the pressure amplitude of the standing wave.

The analogy between the radiation force and the restoring force of a spring can also be used to calculate the distance between the sphere levitation position and the pressure node position, which is denoted by $\Delta z = z_n - z$ in Fig. 2. Therefore, by combining Eqs. (36), (38), and (39), we find

$$\Delta z = \frac{mg}{K} = \frac{4\rho_0\rho_p c_0^2 g}{5k^2 p_0^2} \quad (40)$$

which is valid for small displacements in relation to the pressure node.

When a levitating object is perturbed by an external force, it oscillates around the pressure node. Neglecting damping, this motion can be described by a simple harmonic oscillator, in which the natural angular frequency (Ω) of the sphere oscillation can be calculated by

$$\Omega = \sqrt{\frac{K}{m}} = \sqrt{\frac{5k^2 p_0^2}{4\rho_0\rho_p c_0^2}} \quad (41)$$

which shows that the frequency of the sphere oscillation is proportional to the acoustic pressure amplitude. As an example, Fig. 4 shows the damped oscillatory motion of a 3-mm polypropylene sphere in a single-axis acoustic levitation device formed by a 20.3 kHz ultrasonic transducer and a concave reflector [55]. With the transducer switched off, the sphere was placed on the reflector and a high-speed camera was used to record the vertical oscillatory motion of the sphere immediately after the transducer was switched on. Figure 4 shows that after the transducer is turned on, the sphere oscillates at a frequency of 31 Hz around the pressure node. As described in ref. [55], the frequency of the sphere oscillation can be controlled by altering the pressure amplitude in the acoustic cavity. It is also possible to use the oscillatory behavior of the levitating object to determine the density of different materials, including liquids and solids [56].

2.6 Numerical Determination of the Acoustic Radiation Force

Analytical expressions for the acoustic radiation force are only available for problems with simple geometry, such as a sphere in traveling [57] and standing [58] wave fields, a small sphere in a rectangular, cylindrical and spherical cavities [52], and a sphere in the presence of Bessel [59], focused [60], and vortex [61] beams. However, most levitation devices have complex geometry and the numerical determination of the acoustic radiation force becomes necessary.

Different numerical methods have been applied to calculate the acoustic radiation force on particles and objects, such as the lattice Boltzmann method (LBM) [62, 63], finite-difference time-domain (FDTD) [64], boundary element method (BEM) [4], computational fluid dynamics (CFD) simulations [65–67], and the finite element method (FEM) [46, 50, 68, 69].

A usual approach to obtain the radiation force on objects much smaller than the acoustic wavelength consists in using a numerical method to obtain the incident first-order pressure and particle velocity distributions in the fluid medium and then apply the Gor'kov expression [25] to calculate the potential of the radiation force. This strategy has been adopted by numerous researchers [4, 48–50, 53, 70]. The main advantage of this strategy is that the pressure and velocity fields are simulated without the presence of the object. Another numerical approach, valid for objects of arbitrary shape and size, consists in simulating the first-order pressure and velocity fields around the object and then apply Eq. (24) or (25) to obtain the radiation force on the object. This second strategy has been applied in refs. [5, 46, 65, 68, 71, 72].

In this section, the two approaches above are illustrated by applying the finite element method to calculate the acoustic radiation force that acts on a rigid sphere in an acoustic levitation device. The levitation device is composed of a circular ultrasonic transducer (radius of 10 mm) and a plane reflector (radius of 19 mm), which are separated by a distance (H). It is assumed that the transducer surface vibrates harmonically at a frequency of 25.25 kHz with a velocity amplitude (u_0) of 1 m/s. The air medium is modeled by assuming $c_0 = 343$ m/s and $\rho_0 = 1.2$ kg/m^3. The two axisymmetric models are illustrated in Fig. 5, and they are implemented in the software COMSOL Multiphysics. To avoid wave reflections at the edges of the air domain, perfectly matched layers (PMLs) are employed.

Before determining the acoustic radiation force on the sphere, the numerical model of Fig. 5a is applied to obtain the acoustic radiation force on the reflector as a function of H. This numerical procedure is presented in Section 2.6.1 and is used to find the resonances of the acoustic cavity. In Section 2.6.2, the acoustic radiation force that acts on a small rigid sphere is determined numerically by using the model of Fig. 5a. Finally, Section 2.6.3 shows how the numerical model

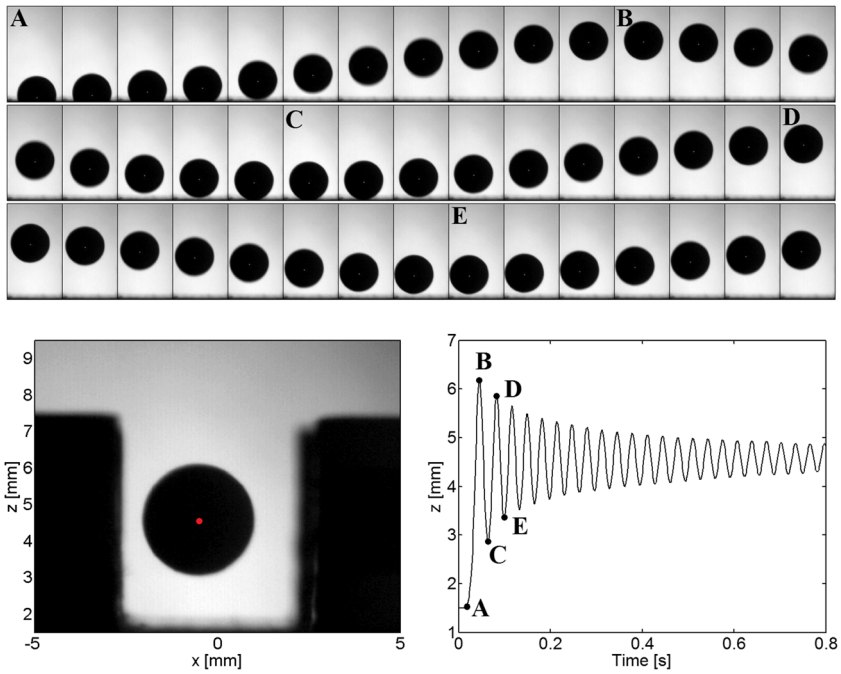

Fig. 4 The top figure shows the oscillatory behavior of a 3-mm polypropylene sphere in a 20.3 kHz single-axis acoustic levitator. The sequence of frames was obtained by a high-speed camera recording at 500 fps immediately after the levitator was switched on. The bottom left figure shows the sphere at its equilibrium position, and the bottom right figure shows the sphere vertical position as a function of time. (Reprinted from [55], with the permission of AIP Publishing)

of Fig. 5b can be applied to find the acoustic radiation force acting on an object of arbitrary shape and size.

2.6.1 Acoustic Radiation Force on the Reflector

The levitation device to be simulated is a resonant device, and consequently, the distance (H) should be adjusted to a resonant state. For a plane standing wave, the resonances occur when H is set to a multiple of a half wavelength. However, as pointed out by Xie and Wei [4], the assumption of a plane wave is not totally valid for a practical levitator, and the resonances occur when H is slightly higher than a multiple of a half wavelength.

In order to find the optimal values of H, the acoustic radiation force exerted on the reflector is calculated as a function of H. To calculate the radiation force, the model of Fig. 5a is applied to obtain the acoustic pressure (p_1) and the particle velocity ($\mathbf{u}_1$) in the air domain. These fields are replaced in Eq. (23) to find the acoustic radiation pressure on the reflector, and the radiation pressure is integrated over the reflector surface to find the acoustic radiation force. This procedure was adopted by Hong and coauthors [68], who showed that the radiation force on the reflector presents a substantial increase at the resonant states of the acoustic cavity. The acoustic radiation force on the reflector as a function of H is presented in Fig. 6. According to Fig. 6, the first resonant state occurs for $H_1 = 7.45$ mm ($H_1 = 0.548\lambda$). The high-order resonances occur at $H_2 = 14.60$ mm ($H_2 = 1.075\lambda$), $H_3 = 21.55$ mm ($H_3 = 1.586\lambda$), and $H_4 = 28.35$ mm ($H_4 = 2.087\lambda$). It can also be observed in Fig. 6 that for small values of H, a high acoustic radiation force on the reflector can be achieved. This region very close to the transducer surface is referred to as a near-field region, and we shall see in Section 3.2 that this force can be used to levitate planar objects above the transducer surface.

2.6.2 Acoustic Radiation Force on a Small Rigid Sphere

After finding the resonances of the acoustic cavity, we can apply the model of Fig. 5a to obtain the acoustic radiation force that acts on a small sphere in an acoustic levitation device. This model is based on the Gor'kov expression, and the potential of the radiation force is calculated from the incident acoustic pressure and velocity fields. Consequently, an acoustic simulation without the presence of the sphere is performed to obtain the fields p_1^{in} and $\mathbf{u}_1^{in}$. These fields are replaced in Eq. (26) to find the Gor'kov potential.

To illustrate this numerical procedure, the model of Fig. 5a was used to calculate the incident fields p_1^{in} and $\mathbf{u}_1^{in}$, which are shown in Fig. 7a, b, respectively. These fields were obtained for the third resonance ($H_3 = 21.55$ mm) of the acoustic cavity and were replaced in Eq. (26) to obtain the potential of the acoustic radiation force that acts on a rigid ($f_1 = f_2 = 1$) sphere of radius $R = 1.5$ mm. The potential is shown in Fig. 7c, and the symbols "+" indicate the positions of minimum potential. In the absence of gravity, small spheres are acoustically trapped at the positions of minimum potential of the radiation force, and in the Earth's environment, the spheres levitate slightly below the trapping points indicated in Fig. 7c. In any case, the trapping positions in a gravitational field can be easily found by summing the Gor'kov potential and the gravitational potential [73].

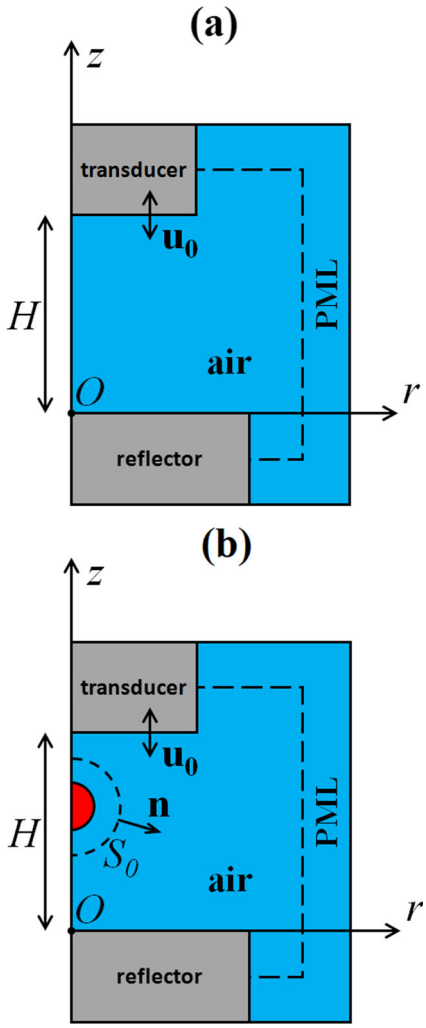

Fig. 5 Axisymmetric models used to calculate the acoustic radiation force on a sphere in an acoustic levitation device. **a** Model based on the Gor'kov expression. **b** Model based on Eq. (25)

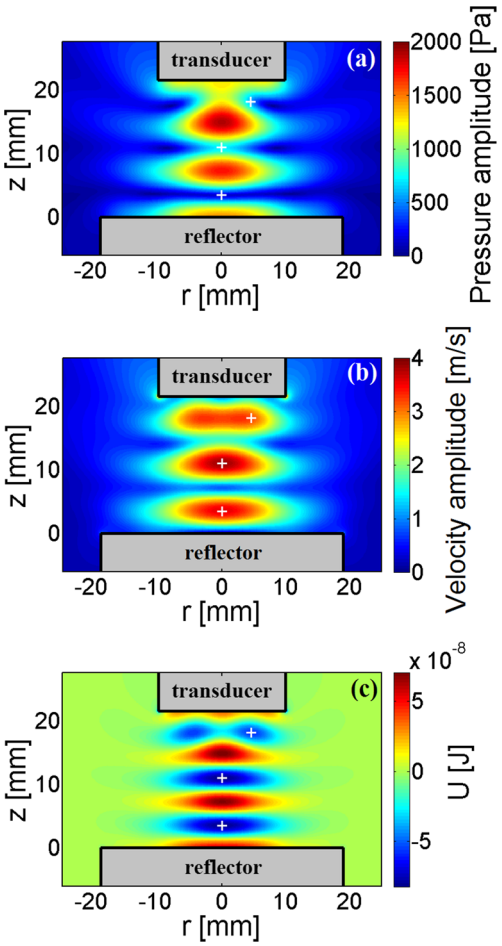

Fig. 7 Simulated fields obtained with the numerical model of Fig. 5a for $H = 21.55$ mm. The transducer surface vibrates harmonically at 25.25 kHz with a velocity amplitude of 1 m/s. **a** Pressure amplitude. **b** Velocity amplitude. **c** Potential of the acoustic radiation force on a rigid sphere of radius $R = 1.5$ mm

The potential of the radiation force along the z-axis of Fig. 7c is shown in Fig. 8a. From this potential, the vertical acoustic radiation force (F_z) is calculated by

$$F_z = -\frac{\partial U}{\partial z}. \tag{42}$$

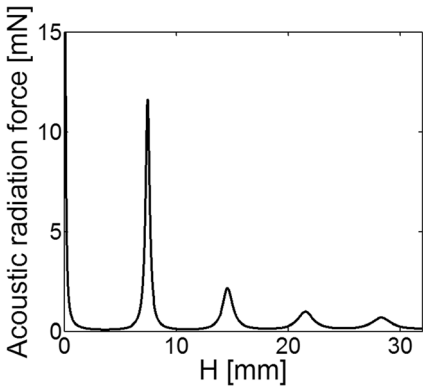

Fig. 6 Simulated acoustic radiation force on the reflector of a levitation device formed by a 25.25 kHz ultrasonic transducer and a plane reflector as a function of H. The radiation force was simulated by using the numerical model of Fig. 5a

The vertical acoustic radiation force along the z-axis acting on a rigid sphere of radius $R = 1.5$ mm is shown in Fig. 8b. By comparing Fig. 8a and (b), we can observe that the acoustic radiation force is zero at the positions of the minimum Gor'kov potential. We can also observe that the force curve of Fig. 8b presents a negative slope at these positions, and for small displacements in respect to the equilibrium position, it can be approximated by a restoring force of a spring.

The comparison between the Gor'kov potential and the levitation positions of small spheres in a single-axis acoustic levitator formed by a 25.25 kHz ultrasonic transducer and a plane reflector is shown in Fig. 9. Figure 9a, b was obtained for the first resonant state of the acoustic cavity ($H_1 =$ 7.45 mm), and Fig. 9c and (d) was obtained for $H_3 =$ 21.55 mm. Figure 9 shows there is a good agreement between

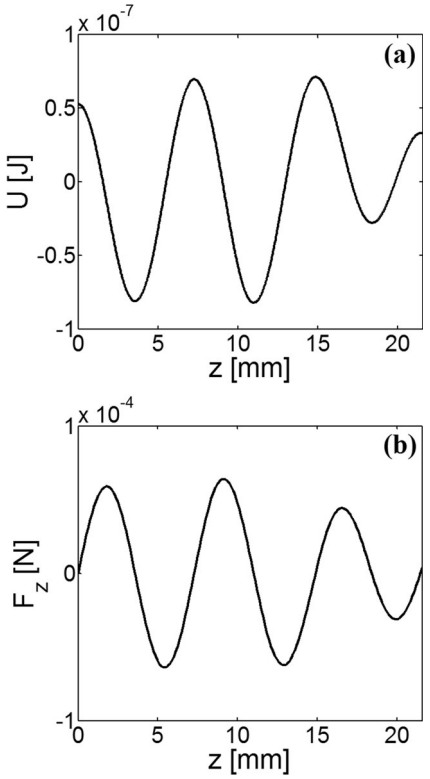

Fig. 8 Gor'kov potential and vertical acoustic radiation force along the z-axis of Fig. 7. **a** Potential of the acoustic radiation force. **b** Vertical force acting on a rigid sphere of radius $R = 1.5$ mm

the positions of the minimum Gor'kov potential and the levitation positions obtained experimentally. In Fig. 9c, d, the upper levitation position is not aligned with the z-axis, meaning that this minimum potential corresponds to a ring-shaped potential well.

In Section 2.5, an analytical expression for the acoustic radiation force that acts on a small rigid sphere in a plane standing wave field, which was useful to calculate the vertical force on a sphere in an acoustic levitation device, was derived. However, a plane wave only provides an axial force to the sphere and a successful levitation requires not only an axial force but also a lateral restoring force to prevent the object from escaping laterally. As discussed by Barmatz and Collas [52], a useful strategy to evaluate the degree of stability of a potential well is to calculate its elastic constants in the vertical and horizontal directions, given by

$$K_z = \frac{d^2U}{dz^2} \tag{43}$$

$$K_r = \frac{d^2U}{dr^2} \tag{44}$$

where K_z is the elastic constant in the vertical direction and K_r is the elastic constant in the radial direction. By analyzing the shape of the potential wells of Fig. 9c, we can conclude that the two bottom potential wells present vertical and horizontal stability. In the case of the top potential well, there is vertical and radial stability, but the object is free to move along the azimuthal direction, since the elastic constant along the azimuthal direction is zero.

2.6.3 Acoustic Radiation Force on an Object of Arbitrary Shape and Size

The acoustic radiation force obtained with the numerical model of Fig. 5a is valid when the sphere radius is much smaller than the acoustic wavelength. For larger spheres, the acoustic radiation force can be determined by the model of Fig. 5b, where the force is calculated by Eq. (25). The comparison between the vertical force obtained by the two models is presented in Fig. 10. For a sphere of radius $R = 0.5$ mm ($R = 0.037\lambda$), the forces provided by both models are very similar. However, when the sphere radius increases to $R = 1.5$ mm ($R = 0.110\lambda$), the radiation force provided by the model based on the Gor'kov expression differs from the model based on Eq. (25).

Although the model of Fig. 5b was applied to obtain the force on a rigid sphere, it is not restricted to spheres and can be applied to obtain the acoustic radiation force on objects of arbitrary shape and size [46]. In addition, the method can be easily extended to obtain not only the force but also the radiation torque that acts on an object [74].

3 Static Acoustic Levitation Methods

In this section, the acoustic levitation methods capable of levitating objects at fixed positions in space are reviewed. The levitation methods capable of manipulating objects are presented in Section 4.

Until recently, acoustic levitation has been classified in only two types: standing wave acoustic levitation and near-field levitation [15]. However, due to the recent advance in acoustic levitation, we now can extend this classification to five types, which are summarized in Fig. 11.

Figure 11a illustrates the well-known standing wave acoustic levitation method. In this method, solid objects and liquid drops of size much smaller than the acoustic wavelength are suspended in the pressure nodes of the standing wave. This method is discussed in detail in Section 3.1.

The second method, shown in Fig. 11b, is the near-field acoustic levitation (also called the squeeze film levitation). In this method, a large plane object levitates slightly above the vibrating surface of a transducer. In general, the object levitates at a height varying from tens to hundreds of micrometers above the transducer surface. This method will be reviewed in Section 3.2.

The third acoustic levitation method is illustrated in Fig. 11c. This method is similar to the near-field levitation,

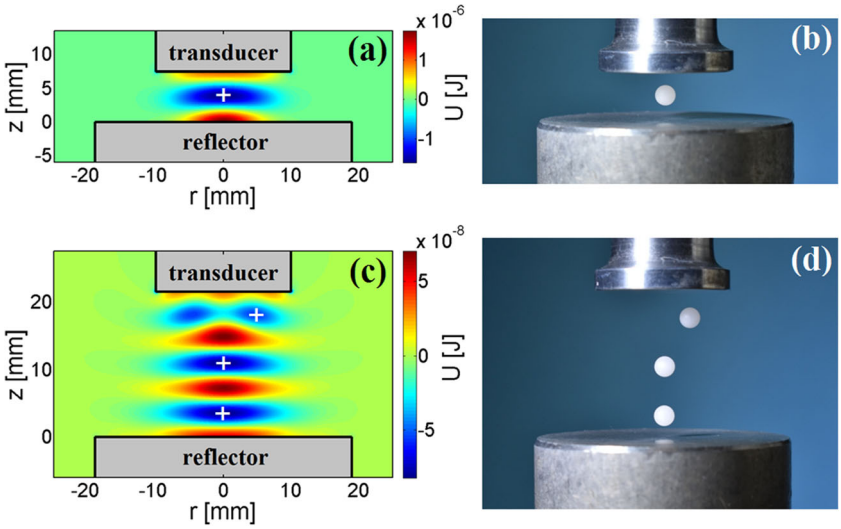

Fig. 9 Comparison between the Gor'kov potential and the levitation positions of polypropylene spheres in a single-axis acoustic levitator. **a** Simulated potential (H_1 = 7.45 mm). **b** Experimental (H_1 = 7.45 mm). **c** Simulated potential (H_3 = 21.55 mm). **d** Experimental (H_3 = 21.55 mm)

but the plane object levitates below the transducer surface. This method is not well known, and there is no specific name to refer to this type of levitation. Due to its similarity to the near-field levitation, we will refer to this technique as inverted near-field levitation.

Figure 11d illustrates the acoustic levitation of a large object at a distance of approximately a half wavelength from the transducer surface. Contrary to the near-field levitation, in this technique, a standing wave is formed between the transducer and the object. In order to differentiate this method from the near-field levitation, we will use the term far-field levitation to refer to this method. The term far-field force was previously adopted by Hong et al. [68], and it seems appropriate to differentiate this method from the near-field levitation method. The far-field acoustic levitation method is described in Section 3.4.

The last acoustic levitation method uses a single beam to levitate particles much smaller than the acoustic wavelength. This method, illustrated in Fig. 11e, is described in Section 3.5.

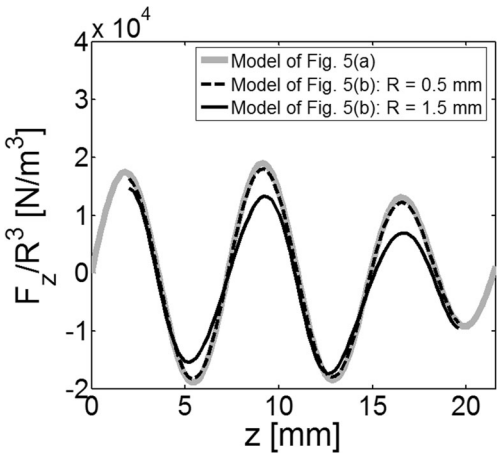

Fig. 10 Simulated vertical acoustic radiation force (F_z) on a rigid sphere using the numerical models of Fig. 5 for the third resonance of the acoustic cavity (H_3 = 21.55 mm)

3.1 Standing Wave Acoustic Levitation

The most common technique to acoustically suspend particles in air is the standing wave levitation method. In this method, solid objects and liquid drops much smaller than the acoustic wavelength are suspended in the pressure nodes of a standing wave field.

The first experimental observation of the trapping of small particles at the pressure nodes of a standing wave was described by August Kundt [75] in 1866. In his experiment, known today as Kundt's tube experiment, an acoustic standing wave was generated inside a horizontal transparent tube by a resonating rod at one end. At the other end, a movable rigid piston was used to adjust the length. When generating an acoustic standing wave in the tube, fine dust particles were agglomerated at the pressure nodes. However, since the agglomerated particles stayed in contact with the tube walls, we cannot say that this was the first acoustic levitation experiment, but the experiment demonstrated the acoustic radiation force on small particles due to a standing wave field.

The first use of acoustic radiation force for levitation is attributed to Bücks and Müller [76] in 1933, when they reported an experiment in which alcohol droplets were suspended at the pressure nodes of a standing wave established between a vibrating quartz rod and a reflector. Since then, numerous acoustic levitation devices [4, 6, 13, 50, 70, 77–104] based on standing waves have been developed. In 1941, St. Clair [77] described an experiment in which small objects such as a small coin and a lead shot were levitated by a high-intensity standing wave field (a picture of the levitating coin can be found in another paper of St. Clair [78]). A few years later, Allen and Rudnick [79] used a powerful

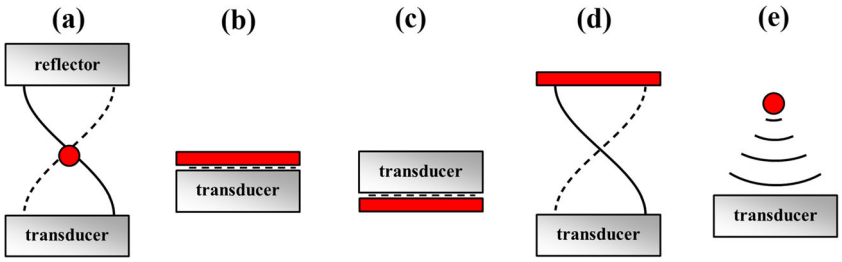

Fig. 11 Acoustic levitation methods. **a** Standing wave acoustic levitation. **b** Near-field acoustic levitation. **c** Inverted near-field levitation. **d** Far-field acoustic levitation. **e** Single-beam levitation

high-frequency siren and a reflector to acoustically suspend coins, small balls, and other small objects. In the following decades, many other investigators developed standing wave levitators with similar characteristics.

In the 1970s and 1980s, the development of new standing wave devices [80, 81, 105, 106] was motivated by the possibility of applying acoustic radiation force for the contactless positioning of materials in microgravity, with many studies [81, 85, 105–108] being conducted under NASA contracts. In 1974, Taylor Wang and collaborators [80] described the development of a rectangular acoustic chamber for positioning molten materials in space. The chamber, measuring 4 in. × 4.5 in. × 5 in., was excited by three orthogonal speakers operating at an audible frequency. In laboratory tests on Earth, the device was able to levitate and to rotate an expanded polystyrene ball, soap bubbles, and water droplets. One decade later, in 1985, Wang flew aboard the Challenger NASA Space Shuttle (mission STS-51B) and used a similar acoustic chamber to investigate the behavior of acoustically rotated free drops in a microgravity environment [109]. The acoustic chamber was used for positioning drops through the action of the acoustic radiation force, and the drops were rotated by using acoustic viscous torques [110].

Another researcher and astronaut who made numerous contributions [35, 56, 85, 111, 112] to acoustic levitation was Eugene Trinh. He flew aboard the Columbia Space Shuttle in 1992 (mission STS-50) and conducted experiments involving the rotation [113] and oscillation [114] of liquid drops. These experiments were performed in the Drop Physics Module (DPM), which basically consists of a rectangular chamber with dimensions 127 mm × 127 mm × 152.4 mm excited by four speakers. Similar to the experiments performed by Wang et al. [109], Trinh used standing waves with the main purpose of centering the liquid drop at the center of the chamber.

In parallel with the studies being funded by NASA in the 1970s and 1980s, the European Space Agency (ESA) has also funded the development of acoustic positioning systems for space applications [84]. These positioning devices initially developed for space applications were later modified to allow levitation of objects in terrestrial environments. The German researcher Ernst-Güenter Lierke [84, 90, 115, 116] played an important role in this process. He developed a variety of acoustic levitation devices to levitate solid objects and liquid drops. His studies in acoustic levitation resulted in commercial acoustic levitators [90] that have been employed in a wide range of experiments [12, 117, 118].

In the literature, two main types of standing wave levitators can be found. The first type is called the single axis [4, 6, 13, 50, 70, 77, 78, 81–85, 90, 91, 93–102, 104], and it basically consists of a transducer and a reflector (or two opposed transducers), in which a standing wave field is established between them. The second type uses a closed resonant chamber [80, 105, 111, 119, 120] to produce a standing wave field in one of the acoustic modes of the cavity.

Single-axis acoustic levitators can be formed by a single transducer and a reflector [4, 50, 81, 82, 85], by two opposing transducers [94] or by two opposing arrays of transducers [104]. They can also be divided in resonant and nonresonant devices. In a resonant device formed by one transducer and one reflector, the separation distance between the transducer and the reflector should be adjusted to one of the resonant modes of the cavity. In the specific case of a plane standing wave, the resonances occur when the distance between transducer and the reflector is set to a multiple of a half wavelength. For the first resonance, illustrated in Figs. 9b and 11a, the standing wave has only one pressure node and, consequently, only one potential well is available for levitation. Yet, the distance between the transducer and the reflector can also be adjusted to a higher-order resonance, allowing the acoustic levitation of multiple spheres at different pressure nodes, as shown in Fig. 9d. Resonant single-axis levitators have been applied to levitate solid materials [50, 70, 81, 96], liquid drops [7, 112], pharmaceutical drugs [14], soap bubbles [121], and even small living animals [9, 10]. One of the main advantages of resonant levitators is that it can achieve high acoustic pressure amplitudes, allowing the acoustic levitation of high-density materials, such as liquid mercury or iridium [122]. As an example, Fig. 12 shows the acoustic levitation of small living animals by a single-axis resonant acoustic levitator formed by a 16.7 kHz transducer and a concave reflector. This levitation experiment was performed by Xie and coauthors [9], who reported that the vitality of the ant and the ladybug was not evidently influenced by the levitation. They also reported that the vitality of the fish was reduced, but they attributed this reduction to the inadequacy of water supply.

The most simple configuration for a single-axis acoustic levitator consists of a plane transducer and plane reflector

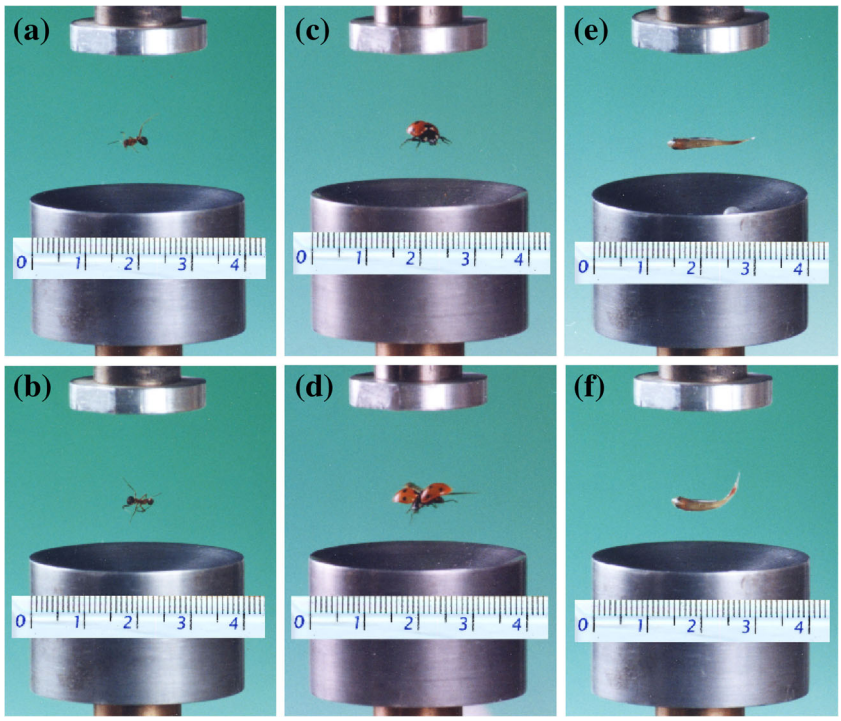

Fig. 12 Acoustic levitation of small living animals by a resonant single-axis device formed by a 16.7 kHz circular transducer with a radiating face of 25 mm in diameter and a concave reflector with a diameter of 40 mm and curvature radius of 40 mm. **a**, **b** A living ant. **c**, **d** A ladybug. The levitation of a small fish is shown in **e**, **f**. (Reprinted from [9], with the permission of AIP Publishing)

[77, 78, 81]. However, it has been found that the use of concave surfaces allows to significantly increase the axial and radial forces on the levitated objects [4, 50, 82, 84, 97]. Therefore, many single-axis levitators are formed by a plane transducer and a concave reflector [70, 84, 90, 91, 98, 101] or by both transducer and reflector having concave surfaces [49, 50, 82, 97, 123]. In addition to levitators employing concave and flat surfaces, the use of reflectors with unusual characteristics has also been reported in the literature [95, 102, 124]. For example, Melde et al. [102] designed the shape of a reflector using a holographic technique and used a 3D printer to fabricate the reflector. When combining the designed reflector with a 100 kHz ultrasonic transducer, they were able to levitate two water drops at the same height, but separated by a distance of 3 mm from the levitator main axis. Another type of reflector with an unusual characteristic was described by Hong and coauthors [95, 124], who used a liquid reflecting surface instead of a traditional solid reflector. Some years later, Foresti et al. [125] employed a similar type of reflector to levitate and to transport high-density materials.

Single-axis acoustic levitators can also be nonresonant and can be formed by one transducer and a reflector [83, 87, 100] or by two opposing emitters [104]. In contrast with a resonant levitator, in which the standing wave is produced by the superposition of the multiple reflected waves between the transducer and the reflector, in a nonresonant levitator, the standing wave is basically formed by the superposition of two counter-propagating waves (the emitted and reflected wave, or the counter-propagating waves emitted by two opposing emitters). The main advantage of the nonresonant levitators is that the separation distance between the transducer and the reflector (or the distance between transducers) can be freely adjusted. Figure 13 shows the acoustic levitation of expanded polystyrene particles by a nonresonant acoustic levitation device formed by a 23.7 kHz transducer with a radiating face of 10 mm in diameter and a concave reflector of 40 mm diameter with a curvature radius of 33 mm [100]. In this device, the transducer is kept at a fixed position and the reflector can be tilted and translated vertically and horizontally. Although the levitator geometry of Fig. 13 is similar to that of a resonant levitator (e.g., Fig. 12), the transducer of Fig. 13 has a small diameter in respect to the wavelength. The small transducer diameter leads to two consequences. The first one is that the transducer emits a nearly spherical wave. The second is that high-order reflections are minimized since the wave energy is almost completely dispersed into the surrounding medium after the first reflection on the reflector surface. In these conditions, we can assume that the standing wave is mainly formed by the superposition of the emitted wave and the first reflected wave.

Recently, Marzo and coauthors [104] presented a single-axis nonresonant acoustic levitator, which was formed by two concave arrays of 40 kHz small transducers. Their levitator is low cost and simple to fabricate. The levitator uses inexpensive 40 kHz transducers, the levitator mechanical parts can be fabricated in a 3D printer, and the transducers are driven by an electronic circuit consisting of an Arduino board and an H-Bridge driver. The authors expect the new levitator will democratize access to acoustic levitation.

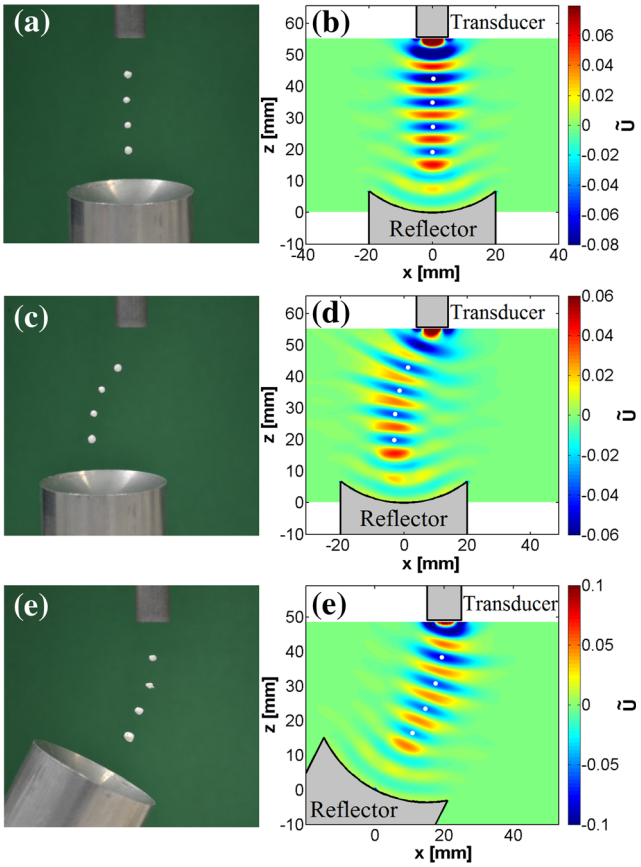

Fig. 13 Acoustic levitation of expanded polystyrene particles by a 23.7 kHz nonresonant acoustic levitator. **a**, **c**, **e** Experimental. **b**, **d**, **f** Simulated Gor'kov potential. (Reprinted from [100], with the permission of AIP Publishing)

3.2 Near-Field Acoustic Levitation

In the standing wave acoustic levitation method, solid objects and liquid drops relatively small in comparison with the acoustic wavelength are suspended at the pressure nodes of a standing wave field. In this levitation method, the maximum weight of the levitated objects is on the order of few milligrams. Another acoustic levitation approach, capable of levitating heavy planar objects, is the near-field acoustic levitation [126–137], which is illustrated in Fig. 11b. In the near-field levitation (also called the squeeze film levitation), a large planar object levitates slightly above the transducer surface, with a thin air layer separating them. In contrast with a typical single-axis levitator, where a standing wave is generated between a transducer and a reflector, in the near-field method, the object itself acts as a reflector. In fact, if we analyze the acoustic radiation force of Fig. 6, we can observe that the acoustic radiation force that acts on the reflector presents a substantial increase when the reflector approaches the transducer surface. Therefore, if the reflector is replaced by the object, we can use the acoustic radiation force to levitate the plane object above the transducer surface. It has already been demonstrated that near-field acoustic levitation is capable of levitating planar objects of several kilograms in weight at a distance of tens to hundreds of micrometers above the transducer surface [131].

Near-field acoustic levitation can be achieved by using a transducer whose surface vibrates uniformly in amplitude and phase [126], but another common strategy is to employ a plate vibrating in a flexural mode [127, 128, 130]. As we will see in Section 4.2, metal plates vibrating in the flexural mode can be used to levitate and to transport large planar objects.

Near-field acoustic levitation is usually employed to levitate planar objects above a vibrating surface [126–134], but it can also be applied to levitate nonplanar objects, such as spheres [138], cylindrical shaped objects [139], and L-shaped beams [135, 140]. It has also been demonstrated that the principle behind near-field acoustic levitation can be applied to control the friction between a vibrating surface and human fingertips [141, 142]. Many researchers [142–144] expect this principle could be applied to touchscreens to give the impression of touching different kinds of surfaces.

3.3 Inverted Near-Field Acoustic Levitation

In the near-field acoustic levitation, illustrated in Fig. 11b, the transducer produces a repulsive acoustic radiation force on the plane object, allowing its levitation slightly above the transducer surface. It has also been reported in the literature that, in some conditions, the repulsive force can change from repulsive to attractive [129, 145]. In this case, the transducer radiating face can be pointed downwards and a plane object can be levitated slightly below the transducer radiating face [146–149], as shown in Fig. 11c. Similar to the near-field levitation, a thin layer of air separates the object from the transducer. As there is no established name for this type of levitation, we will refer to this method as "inverted near-field acoustic levitation."

Figure 14 shows the acoustic levitation of a small disk using the inverted near-field acoustic levitation method. In this figure, Takasaki et al. [146] used a 21 kHz bolt-clamped Langevin-type transducer to levitate a disk of 3 mm in diameter and 0.5 mm in thickness slightly below the transducer radiating face. As it can be observed in Fig. 14, there is a small air gap between the transducer and the object.

At the moment, there is no established model to predict the radiation force acting on the object when it levitates slightly below the transducer surface, but the experimental results from the literature [145, 149] suggest that a repulsive force between the transducer and the object occurs when the transducer and the object have large diameters in respect to the acoustic wavelength. The literature [146, 149] also suggests that when the transducer and the object have small diameters in comparison with the wavelength, the radiation force is attractive. Therefore, we can expect there should be a specific

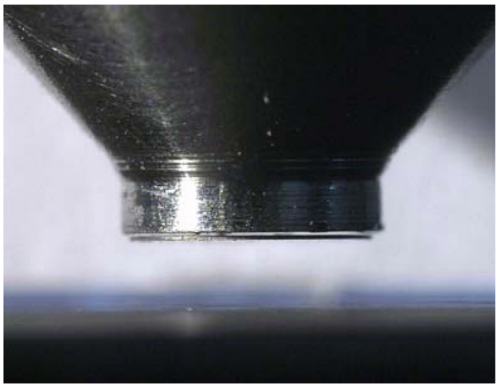

Fig. 14 Acoustic levitation of a disk of 3 mm in diameter and 0.5 mm in thickness slightly below an ultrasonic transducer operating at 21 kHz. (Reprinted from [146], Copyright 2010, with the permission from Elsevier)

diameter in respect to the wavelength where the force changes from repulsive to attractive. It is also important to note that in the inverted near-field acoustic levitation, the object does not touch the transducer. This means that when the object is very close to the transducer surface, the radiation force should be repulsive, changing to attractive when it reaches a certain separation distance from the transducer surface.

By analyzing the experimental results of Ueha [145] and assuming that the transducer and the object have the same diameter, it seems that the change from attractive to repulsive force occurs when the ratio between the transducer diameter and the acoustic wavelength is approximately 0.75. Therefore, in contrast with the near-field levitation, where larger planar objects levitate above the transducer surface, in the inverted near-field levitation, small planar objects can be levitated below the transducer face.

3.4 Far-Field Acoustic Levitation

The far-field acoustic levitation method is illustrated in Fig. 11d. This method can be used to levitate objects larger than the acoustic wavelength, and it relies on producing an acoustic standing wave between the object surface and one or more transducers. As shown in Fig. 6, when the distance between the transducer and the object is set to a resonance state, the acoustic radiation force on the object can be substantially increased. This increase of the acoustic radiation force was described by St. Clair in 1941, when he wrote: "The pressure exerted against a metal plate or any other good reflector is astonishing when it is held in such a position as to set up a standing wave field between it and the vibrator." [77]. Despite this description, St Clair used his apparatus to levitate small objects at the pressure nodes of the standing wave, as in Fig. 11a, and there is no evidence that St. Clair used this force to levitate objects larger than the acoustic wavelength.

In 1975, when describing a single-axis levitation device formed by a 20 kHz transducer and a plane reflector, Whymark [81] briefly reported the levitation of a brass disk of 50 mm in diameter by 0.5 mm in thickness. In one of his experiments, the reflector of the levitation device was replaced by the brass disk, which was successfully levitated at a distance of approximately half a wavelength from the transducer surface. From the literature, this seems to be the first time an object larger than the acoustic wavelength was levitated.

In 2011, Zhao and Wallaschek [150] used the same strategy to levitate a compact disk (CD). In their experiment, a 19 kHz Langevin-type transducer connected to a circular metal plate of 120 mm in diameter produced an acoustic standing wave of half a wavelength between the CD and the radiating metal plate. However, their system produced only a vertical force on the CD and the radial stability was achieved by using a central pin in contact with the CD.

In order to solve the problem of horizontal stability, Andrade et al. [5] employed three 25 kHz transducers in a tripod arrangement to levitate an expanded polystyrene sphere of 50 mm in diameter. In this configuration, shown in Fig. 15, each transducer generates an acoustic standing wave between the sphere and the transducer face, providing an axial radiation force on the sphere. By combining three transducers in a tripod configuration, vertical and horizontal stability can be achieved, allowing the levitation of an object larger than the acoustic wavelength.

Recently, the far-field acoustic levitation method was applied to levitate a large object consisting of a human figure made of cardstock paper attached to a slightly curved sheet of 170 mm in length and 71 mm in width [151]. As illustrated in Fig. 16, the object was levitated by a device formed by an aluminum vibrating plate of 300 mm in length and two 25 kHz Langevin-type transducers, which were attached to the ends of the aluminum plate. In this device, the transducers generate a flexural standing wave along the plate. When the curved object is placed at a distance corresponding to half a wavelength from the aluminum plate, an acoustic standing wave is established between the plate and the object, providing an acoustic radiation force capable of suspending the object in air. It was also demonstrated numerically that the curvature of the object is responsible for producing of a horizontal radiation force, which provides horizontal stability to the object.

3.5 Single-Beam Levitation

In the standing wave acoustic levitation method, at least two opposing acoustic elements (i.e., two opposing transducers, or a transducer and an opposing reflector) are required, meaning that the particle should be confined between them. Recently, a new acoustic levitation method, called the single-beam levitation (also called the single-beam trapping), has been demonstrated [53, 152–155]. In this method, small objects are

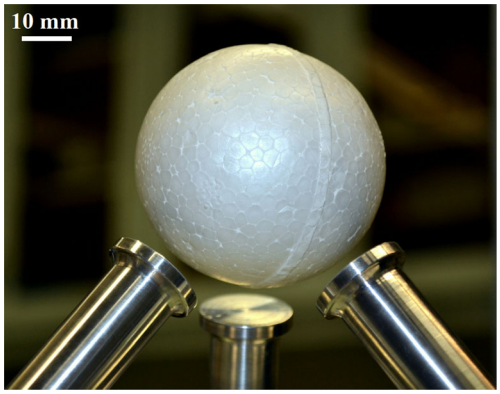

Fig. 15 Acoustic levitation of an expanded polystyrene sphere of 50 mm in diameter using three 25 kHz ultrasonic transducers. (Reprinted from [5], with the permission of AIP Publishing)

acoustically levitated by using a single-sided emitter, as illustrated in Fig. 11e.

The single-beam trapping was first demonstrated in liquid medium when Lee et al. [152] used a 30 MHz focused transducer to trap a lipid droplet at the transducer's focal point. However, the acoustic trapping was only achieved in the transverse direction and the axial particle motion was constrained by a thin film. The simultaneous axial and transverse trapping was demonstrated by Baresch et al. [153], who employed a transducer array driven at 1.15 MHz to trap polystyrene beads in water medium.

The first experimental demonstration of the single-beam levitation in air was reported by Marzo et al. [53]. In their study, they employed single-sided arrays of transducers to acoustically levitate and to manipulate small objects. In one of the arrangements, shown in Fig. 17, they used an 8 × 8 array of 40 kHz transducers of 10 mm in diameter. Using a custom-made electronic board, they were able to control the phase of each transducer independently. In order to find the optimal phase delays for each transducer, they used an optimization algorithm in such a way to produce maximum trapping forces

Fig. 16 Acoustic levitation of a slightly curved object by a levitation device consisting of two 25 kHz transducers attached to an aluminum plate of 300 mm in length. (Reprinted with permission from [151]; Copyright 2017, Acoustic Society of America)

in the desired location. Depending on the phase distribution, they could generate three main types of acoustic traps: twin, vortex [61], and bottle [72] traps. The acoustic radiation force produced by vortex and bottle beams has been previously investigated by other authors [61, 72], but this was the first time these fields have been applied to levitate small objects in air medium. In addition to the vortex and bottle beams, the authors [53] introduced the twin beam, which was successfully applied to generate twin traps and to levitate small particles in mid-air. The twin beam is illustrated in Fig. 17a. The twin beam is characterized by two nearly cylindrical regions of high acoustic pressure amplitude around the object. The twin beam produces an acoustic radiation force that moves the object to the position of minimum acoustic pressure amplitude (i.e., to the region located between the two nearly cylindrical regions). According to the authors [53], the horizontal force between the two cylindrical regions is caused by the pressure amplitude gradient, while the forces in the other two axes are attributed to the velocity gradient. In Fig. 17b, the same array transducer was used to generate a vortex beam, which transfers orbital angular momentum to the levitated object. The same paper also demonstrated the acoustic manipulation of the levitated object (Fig. 17c), which will be covered in Section 4.3.

The single-beam acoustic levitation demonstrated by Marzo et al. [53] requires a complex electronic system to excite each transducer independently, restricting its use to a few research groups. A simplified version of the previous single-beam device was presented shortly thereafter [154]. The new device employed a similar transducer array, but instead of using a complex electronic system to generate the phase delays, the authors used an Arduino board and acoustic delay lines to generate the twin trap. The new single-beam device is portable and can be assembled with components that can be easily found by the general public. In addition, the authors also provided all the steps to create the simplified version of the single-beam acoustic levitation device [154].

In a recent study, Memoli et al. [155] used a collection of metamaterial bricks in front of an 8 × 8 array of 40 kHz transducers to shape the acoustic field. In this study, 16 types of bricks, corresponding to phase delays varying from 0 to $15\pi/8$ in steps of $\pi/8$, were manufactured using a 3D printer. In one of the experiments, they arranged the material bricks to generate a bottle beam to levitate a polystyrene bead in mid-air (Fig. 18b). Pictures of the metamaterial bricks and the mounting frame structure are shown in Fig. 18a.

4 Acoustic Manipulation and Transport of Levitated Objects

From the first acoustic levitation experiments reported in 1933 [76] to the beginning of this century, the progress of

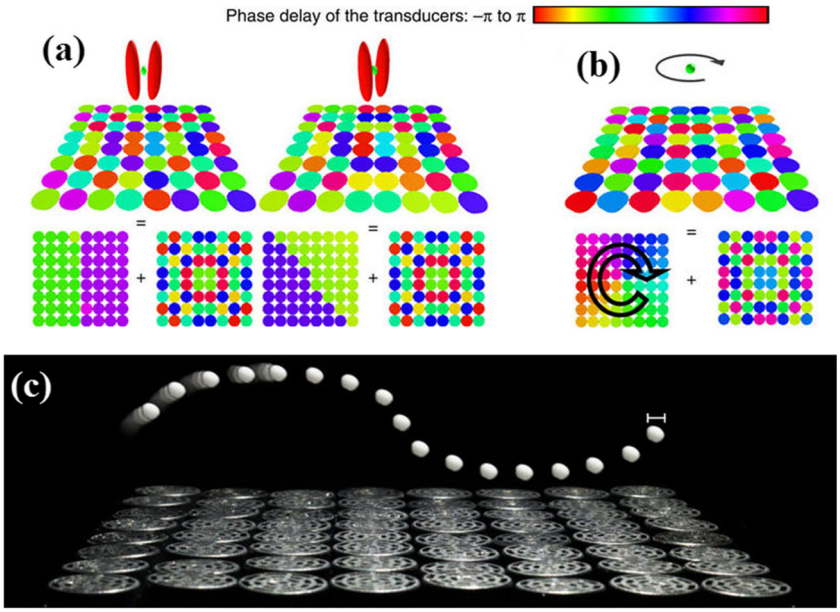

Fig. 17 Acoustic levitation of small objects using the single-beam acoustic levitation. The acoustic beams are generated by an 8 × 8 array of 40 kHz ultrasonic transducers. The colored circles represent the transducers and their corresponding phase delay. **a** Acoustic pressure isosurfaces of a twin beam. **b** Phase distribution used to generate a vortex beam. The vortex beam can transfer orbital angular momentum to the levitated object, thus inducing its rotation. **c** Acoustic levitation and manipulation of the levitated object. (Adapted from [53], licensed under CC BY 4.0)

acoustic levitation was relatively slow. In this period, acoustic levitation methods were almost limited to static experiments, in which small objects and liquid drops could be levitated at fixed positions in space. It is true that in the first levitation devices, object manipulation could be achieved by moving the whole assembly, but this strategy has the inconvenience of requiring moving parts. Although the first strategies to acoustically levitate and to manipulate objects without moving parts were reported three decades ago [111, 120], they had limited manipulation capability, and it was only in the last years that acoustic levitation devices capable of manipulating objects in 3D have been developed.

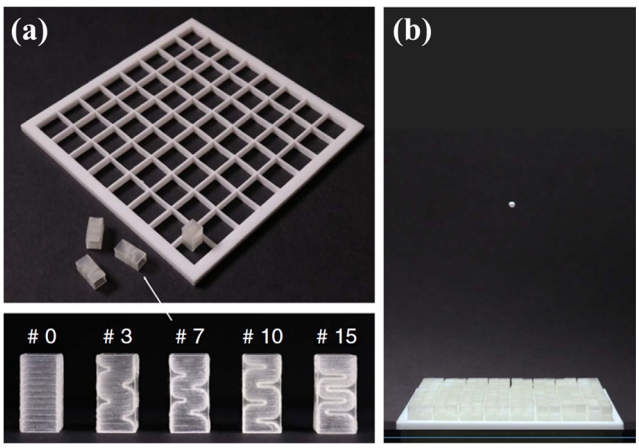

Fig. 18 Single-beam acoustic levitation using a collection of metamaterial bricks in front of an array of 40 kHz transducers. **a** Mounting frame structure and a picture of the manufacture metamaterial bricks. **b** Acoustic levitation of a polystyrene bead using an acoustic bottle beam. (Adapted from [155], licensed under CC BY 4.0)

This section describes how the standing wave, near-field, and single-beam levitation methods can be extended to allow the manipulation and the transport of levitated objects in air.

4.1 Manipulation by the Standing Wave Acoustic Levitation Method

The first studies involving the acoustic manipulation of objects were driven by the possibility of performing the contactless processing of materials in microgravity [106]. In comparison with the Earth's environment, the acoustic manipulation inside a spacecraft requires acoustic forces considerably smaller than the gravitational force. Therefore, it is not surprising that the first acoustic manipulation studies were conducted with the purpose of manipulating objects in a microgravity environment.

In 1975, Fletcher et al. [105] presented an acoustic method for the contactless manipulation of objects inside a resonant rectangular chamber. Similar to the resonant chamber developed by Wang et al. [80], an acoustic standing wave is generated by three orthogonal speakers. The chamber has one movable wall, and the pressure node is located at the center of the chamber, as shown in Fig. 19. As the acoustic radiation force keeps the object at the pressure node, the contactless manipulation can be achieved by displacing the movable wall and, at the same time, changing the frequency of the opposite speaker such that the resonance of the acoustic cavity is maintained. Therefore, by moving the wall by a certain distance, the object is displaced by one half of the distance of the movable wall.

The acoustic manipulation method shown in Fig. 19 requires a movable wall. A different method to manipulate the levitated object inside a rectangular chamber is the mode switching (also called frequency switching), which was

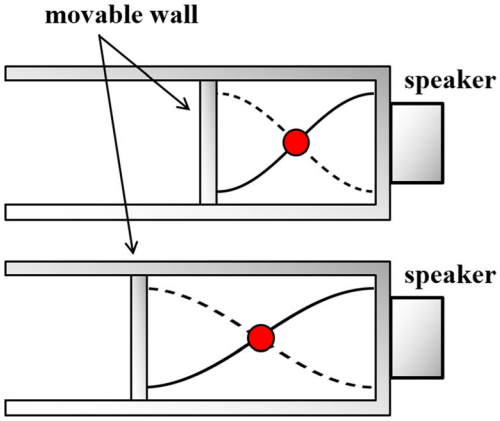

Fig. 19 Acoustic manipulation method proposed by Fletcher et al. [105]. The contactless manipulation along the horizontal direction is achieved by displacing the movable wall and by controlling the frequency of the opposite speaker

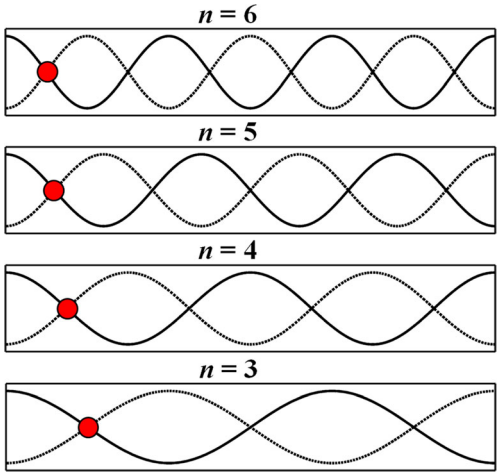

Fig. 20 Acoustic manipulation by using the mode-switching approach [111]. The object is transported by switching between different normal modes of the acoustic cavity

presented by Trinh et al. [111] in 1986. This method does not require moving parts and the 1D manipulation is achieved by switching between different modes of the acoustic cavity, as illustrated in Fig. 20. Trinh et al. [111] demonstrated this approach by transporting a platinum-coated hollow quartz sphere inside a rectangular chamber. This approach was proposed with the objective of manipulating substances from a low-temperature zone to a region of high temperature inside a rectangular chamber in microgravity.

Another method proposed to manipulate objects in microgravity uses a nonresonant acoustic levitator formed by a sound emitter and a small reflector [83, 87]. In this method, the superposition of the incident and reflected waves on the reflector produces an acoustic standing wave, allowing the acoustic levitation of the object at a pressure node located at a distance of approximately a quarter of a wavelength from the reflector surface. Due to the small size of the reflector, high-order reflections are minimized and the acoustic radiation force on the object is almost independent of the separation distance between the emitter and the reflector. In this condition, the levitated object can be manipulated by moving the reflector. A nonresonant acoustic levitation device based on this manipulation method was presented recently [100] and is illustrated in Fig. 13. In this device, the manipulation of the levitated particles is achieved by translating the reflector in respect to the transducer.

Acoustic waves can be used not only to translate levitating objects but can also be applied to rotate objects through the action of acoustic viscous torques [110, 156]. Acoustic viscous torques on the levitated object can be generated by two orthogonal standing waves inside a rectangular resonant chamber [107, 108]. As demonstrated theoretically by Wang and Busse [110], the torque on the object is maximum for a phase shift of 90° between the orthogonal waves. Experiments involving acoustic viscous torques were already carried out on Earth [156] and also in a microgravity environment [109, 113].

Another approach to acoustically manipulate levitating objects consists in generating an acoustic standing wave by the superposition of the traveling waves emitted by two opposed transducers [157, 158]. In this approach, the pressure node positions and, consequently, the levitation positions are altered by changing the relative phase between the transducers. Ideally, the traveling wave emitted by one transducer must not be reflected by the opposed transducer, because the reflections can disrupt the manipulation capability [159]. In practice, a successful manipulation can be achieved by reducing the reflections below a certain limit. According to Grinenko et al. [159], the manipulation by counter-propagating waves can be achieved when the reflection coefficient of the opposed transducer is lower than 0.5.

The translation of the levitated objects by changing the relative phase between transducers has been demonstrated by different authors. In 1995, Matsui et al. [160] reported the vertical translation of small particles in a device consisting of two opposed 20 kHz transducers. In 2007, Kozuka et al. [161] used two tilted transducers to manipulate expanded polystyrene particles in mid-air. In 2009, Weber et al. [94] described the construction of a single-axis acoustic levitator formed by two 22 kHz transducers with a radiating face of approximately 70 mm in diameter. In this levitator, unwanted reflections were reduced by bonding an absorbing material in front of the transducers. The authors also reported that the levitating objects can be displaced vertically by changing the relative phase between the transducers. Recently, Marzo et al. [104] developed a low-cost single-axis levitator that can transport the levitating objects upwards and downwards.

In 2010, Koyama and Nakamura [162, 163] proposed a new type of acoustic levitation system to transport small objects and liquid droplets. The proposed system consists of linear [162] and circular [163] transporters and could be applied to transport objects over large distances. Their linear

acoustic transporter [162] is formed by a long aluminum plate attached to a 22.5 kHz Langevin-type transducer at each end. A planar reflector with the same dimensions of the aluminum plate is positioned at a distance corresponding to one acoustic wavelength from the aluminum plate. When the transducers are electrically excited, a flexural standing wave is generated along the plate. The plate vibration generates an acoustic standing wave in the air gap between the reflector and the plate, in which small objects can be acoustically levitated at the pressure nodes. When the relative phase between the transducers is altered, the levitated objects are transported. The circular transporter [163] presents a similar working principle and is formed by a circular aluminum plate attached to a piezoelectric ring and a reflector. The electrodes of the piezoelectric ring were divided into 24 parts, and by controlling the electrical signals at each electrode, the authors were able to transport small objects in a circular trajectory in steps of 7.5°. The linear transport of levitated objects has also been performed by devices using flexural traveling waves [164] and flexural standing waves in a ring-shaped structure [165]. The concept behind the linear transport was also extended to allow the object manipulation in two dimensions [166].

Bjelobrk et al. [67] demonstrated the contactless transport of levitated objects by using a device consisting of a transducer connected to an aluminum radiating plate and a reflector with cylindrical concavity. The authors investigated their device numerically and found that the horizontal positions of the minimum Gor'kov potential change with the separation distance between the radiating plate and the reflector. Therefore, by controlling the reflector height, the authors demonstrated the horizontal transport of a small polystyrene particle over a distance of 37 mm. In 2012, Bjelobrk et al. used the same device to transport and to merge liquid droplets in air [167].

An important step in the contactless manipulation of levitated objects was made by Foresti et al. [48] in 2013, when they presented a flexible acoustic levitation system able to transport and to merge multiple droplets in air. Their system can also be rearranged to allow the levitation and the rotation of elongated thin objects in a controllable manner. Figure 21 illustrates the working principle of their acoustic manipulation system. In the configuration of Fig. 21, the system comprises five Langevin-type transducers with a square radiating face and a plane reflector, which are positioned at a distance corresponding to half a wavelength from the transducers. The transducers are excited at a frequency of 24.3 kHz, and the voltage amplitude of each transducer can be controlled independently. In the configuration of Fig. 21, the system is used to transport and to merge two liquid droplets in air. At time instant $t = 0$, only the first and the fifth transducers are electrically excited, generating an acoustic standing wave above the corresponding transducers. Then, two liquid droplets are inserted in the levitation system, as illustrated at the top of Fig. 21. At this time instant, the droplets levitated statically

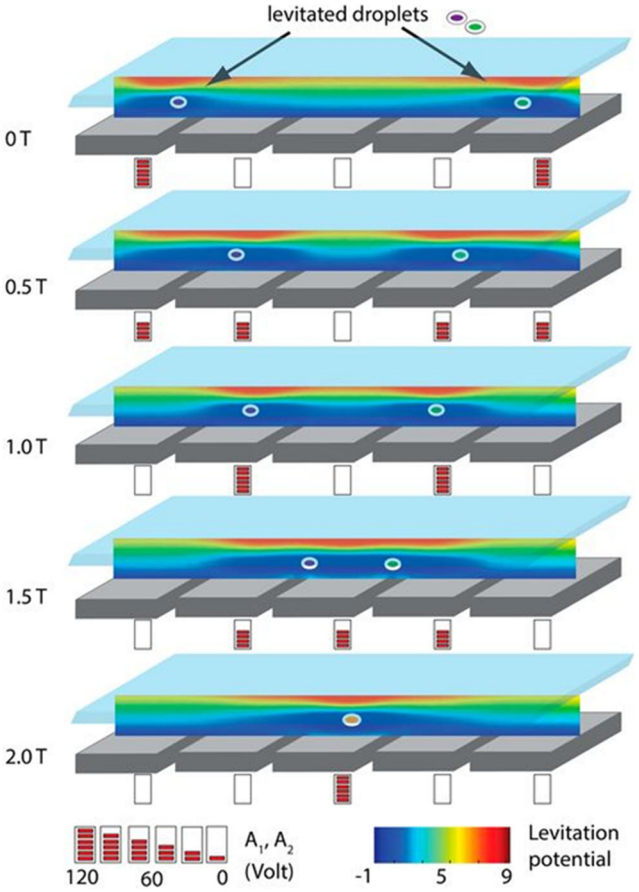

Fig. 21 Acoustic levitation method to transport and to merge liquid droplets in air. The manipulation is achieved by controlling the voltage amplitude of each transducer (Reproduced with permission from [48])

above the transducers. A levitating droplet is transported through the gradual increase of the voltage amplitude of an adjacent transducer while reducing the amplitude of the actual transducer, as illustrated in Fig. 21. Then, after a travel period (T) (the authors defined the travel period (T) as the time required for the object to travel from one transducer to the adjacent transducer [48]), the droplets levitates above the second and fourth transducers (see Fig. 21 at time instant $t = 1.0T$). This procedure is repeated until the two droplets merge at time instant $t = 2.0T$. Figure 21 also shows the levitation potential, which is defined as the sum of the Gor'kov potential and the gravitational potential [48]. As observed in Fig. 21, the droplets follow the positions of minimum levitation potential. Therefore, by controlling the positions of minimum potential, the levitating droplets can be manipulated.

Foresti and coauthors [125] extended the manipulation concept of Fig. 21 to levitate high-density materials. In this new study, they employed Langevin-type transducers with a concave radiating face and used a deformable reflector formed by a prestressed membrane over the surface of a liquid. With this new approach, they were able to transport a steel sphere of 5 mm in diameter. Foresti and Poulikakos [49] also described

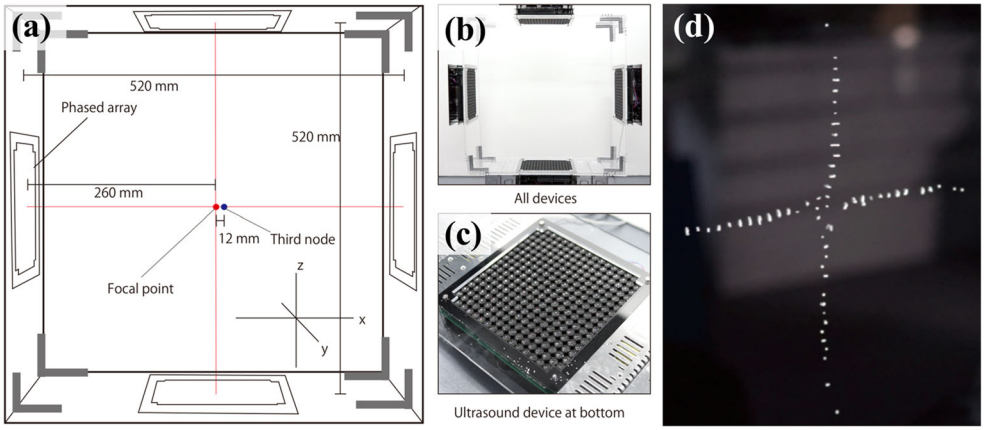

Fig. 22 Acoustic manipulation system developed by Ochiai et al. [168]. **a** Illustration of the manipulation system composed of four arrays of 40 kHz ultrasonic transducers. **b** Photograph of the manipulation system. **c** Array composed of 285 ultrasonic transducers of 40 kHz. **d** Levitating particles. (Adapted from [168], licensed under CC BY 4.0)

an experiment in which six Langevin-type transducers arranged radially were used to levitate and to rotate small objects and liquid droplets in air.

Another important step in acoustic manipulation was made by Ochiai, Hoshi, and Rekimoto [168–170], who developed an acoustic levitation system to manipulate objects in three dimensions. Their system is formed by four arrays of transducers, arranged according to Fig. 22a, b. Each array, shown in Fig. 22c, is formed by 285 transducers arranged in a 170 × 170 mm^2 square area. The transducers operate at a frequency of 40 kHz, and a custom-made electronic circuit allows controlling the phase delay of each individual transducer. The excitation of each transducer can be controlled such that the emitted waves arrive in the phase at the desired focal point. In the neighborhood of the focal point, there is a series of pressure nodes that can be used for levitating small objects (Fig. 22d). By controlling the position of the focal point, the levitating objects can be manipulated in three dimensions (the reader is strongly advised to watch the supporting video of ref. [168]). Using a similar strategy, Omirou et al. [171] presented a modular levitation system composed of two opposed arrays of 40 kHz ultrasonic transducers. In this system, the 3D acoustic manipulation is achieved by controlling the amplitudes and phase of the transducers. Recently, two arrays of 40 kHz have been used to levitate and transport food, offering a new kind of culinary experience [172].

4.2 Object Transport by the Near-Field Acoustic Levitation Method

The near-field acoustic levitation method can be used not only to suspend planar objects above the transducer surface, but it has also been shown that it can be applied to transport heavy planar objects slightly above a vibrating plate [128, 131]. Figure 23 illustrates the near-field acoustic levitation transportation system developed by Hashimoto et al. [128]. This system consists of two 19.5 kHz transducers attached to a metal plate. One transducer generates a traveling flexural wave

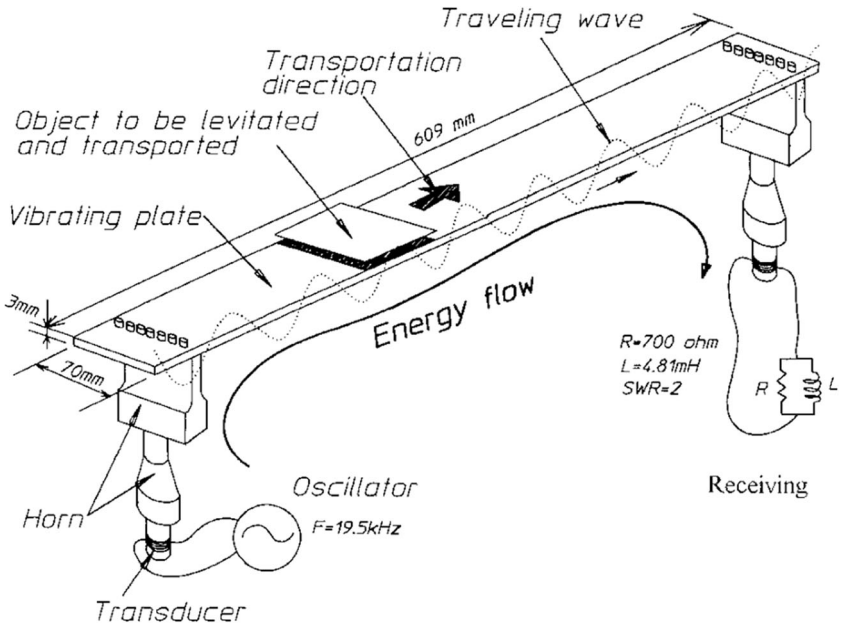

Fig. 23 Near-field acoustic levitation transportation system developed by Hashimoto et al. [128]. In this system, a larger planar object is transported by a flexural traveling wave. (Reprinted with permission from [128], Copyright 1998, Acoustic Society of America)

along the plate while the opposite transducer absorbs it. The near-field transportation system was used to levitate and transport a bakelite plate (90 mm long and 65 mm wide and weight of 8.6 g) with a velocity of 0.7 m/s.

In 2001, Reinhart and coauthors [132] presented a transportation system similar to that proposed by Hashimoto et al. [128]. The system developed by Reinhart and coauthors was used to levitate and to transport 200-mm silicon wafers. The authors also developed another system based on near-field acoustic levitation that was used to load and to unload silicon wafers from wafer cassettes.

Instead of using vibrating surfaces to levitate passive planar objects, the levitating object can also act as a transducer, inducing its own levitation and transport [173–176]. As an example, Fig. 24 shows the self-running levitation device developed by Chen et al. [176]. This device consists of a pair of piezoelectric rings prestressed between a mass block and a bottom plate. The electrodes were divided into four pieces, with each piece corresponding to one quarter of a circle. When the four electrodes are excited in phase at a frequency of 21 kHz, the device vibrates in its longitudinal mode (Fig. 24b), and the device floats against the flat surface. However, when the electrodes are excited at the same frequency but with different phases, the longitudinal mode couples with the bending mode, producing an elliptical vibration of the bottom plate. This vibration causes the object to levitate and to move horizontally. It was also demonstrated that a 2D horizontal motion can be achieved by controlling the relative phases between the electrodes.

4.3 Manipulation Using the Single-Beam Acoustic Levitation Method

The single-beam acoustic levitation method can also be used to manipulate the levitated objects. When demonstrating the acoustic levitation of small objects using single beams in air, Marzo et al. [53] also described a method to manipulate the levitated objects. Manipulation was achieved by changing the phase delays of each individual transducer of a single-sided transducer array. The levitation and manipulation of a small object is illustrated in Fig. 17c.

5 Summary and Future Perspectives

In this article, we started with a brief review of the theory, showing how the governing equations of fluid dynamics can be combined to obtain the linear wave equation and the acoustic radiation pressure. The radiation pressure can be integrated over the object surface to obtain the acoustic radiation force that acts on this object. For the particular case of an object much smaller than the acoustic wavelength, the acoustic radiation force can be calculated with the Gor'kov expression, which considerably simplifies the problem of finding the acoustic radiation force. A simple expression for the acoustic radiation force on a small rigid sphere in a plane standing wave was also presented, and it was shown how linear acoustic simulations can be employed to obtain the acoustic radiation force acting on objects of arbitrary shapes and sizes.

We also presented different acoustic levitation methods that are able to suspend objects in mid-air. Historically, acoustic levitation has been classified in standing wave acoustic levitation and near-field acoustic levitation. But due to the recent advances in acoustic levitation, we believe this classification can now be extended to five types: standing wave, near-field, inverted near-field, far-field, and single-beam acoustic levitation methods. In addition, it has been demonstrated that the standing wave, near-field, and single-beam acoustic levitation methods can also be employed to manipulate the levitated objects.

To conclude, we would like to answer the following question: What is the future of acoustic levitation? Although a significant progress has been made in the last years, we believe that most of the progress is still to come. Functionalities

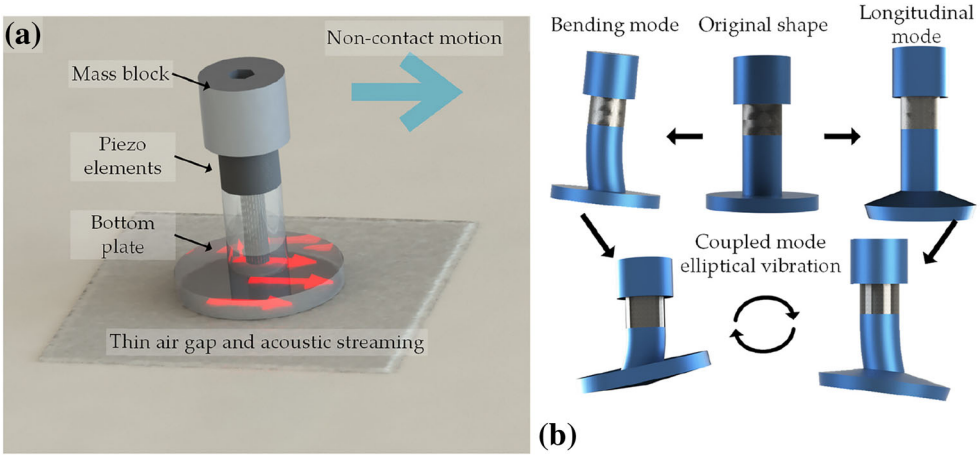

Fig. 24 **a**, **b** Self-running levitation device developed by Chen et al. [176]. A 2D motion is achieved by exciting the piezoceramic electrodes with different phases. (Reprinted from [176], with the permission of AIP Publishing)

such as the ability to manipulate and rotate multiple objects will have a significant impact on acoustic levitation systems. Perhaps, in the future, many of the tasks currently done by robots could be performed by an array of speakers, which could be used to levitate and manipulate objects without any contact. In the future, we can imagine a world where we will have factories in which the objects will be entirely manipulated by sound. We also believe that acoustic levitation has the potential of replacing test tubes, allowing chemical substances to be manipulated by sound. We hope that in the future, acoustic levitation methods will be used for manufacturing new products in space. Another possibility is to combine acoustic levitation with electroencephalography, allowing people to levitate and manipulate objects with their mind.

References

1. C. Columbus, Harry Potter and the Philosopher's Stone (Warner Bros., 2001), This reference is the Harry potter movie: https://en.wikipedia.org/wiki/Harry_Potter_and_the_Philosopher%27s_Stone_(film)
2. E.H. Brandt, Science **243**, 349 (1989)
3. E.H. Brandt, Nature **413**, 474 (2001)
4. W.J. Xie, B. Wei, Phys. Rev. E - Stat. Nonlinear, Soft Matter Phys. **66**, 26605 (2002)
5. M.A.B. Andrade, A.L. Bernassau, J.C. Adamowski, Appl. Phys. Lett. **109**, 1 (2016)
6. A.R. Hanson, E.G. Domich, H.S. Adams, Rev. Sci. Instrum. **35**, 1031 (1964)
7. A.L. Yarin, M. Pfaffenlehner, C. Tropea, J. Fluid Mech. **356**, 65 (1998)
8. D. Zang, Y. Yu, Z. Chen, X. Li, H. Wu, X. Geng, Adv. Colloid Interf. Sci. **243**, 77 (2017)
9. W.J. Xie, C.D. Cao, Y.J. Lü, Z.Y. Hong, B. Wei, Appl. Phys. Lett. **89**, 214102 (2006)
10. M. Sundvik, H.J. Nieminen, A. Salmi, P. Panula, E. Hæggström, Sci. Rep. **5**, 13596 (2015)
11. S. Santesson, S. Nilsson, Anal. Bioanal. Chem. **378**, 1704 (2004)
12. F. Priego-Capote, L. de Castro, TrAC - Trends Anal. Chem. **25**, 856 (2006)
13. J. Gao, C. Cao, B. Wei, Adv. Space Res. **24**, 1293 (1999)
14. C.J. Benmore, J.K.R. Weber, Phys. Rev. X **1**, 11004 (2011)
15. V. Vandaele, P. Lambert, A. Delchambre, Precis. Eng. **29**, 491 (2005)
16. T. Laurell, F. Petersson, A. Nilsson, Chem. Soc. Rev. **36**, 492 (2007)
17. X. Ding, P. Li, S.-C.S. Lin, Z.S. Stratton, N. Nama, F. Guo, D. Slotcavage, X. Mao, J. Shi, F. Costanzo, T.J. Huang, Lab Chip **13**, 3626 (2013)
18. H. Bruus, J. Dual, J. Hawkes, M. Hill, T. Laurell, J. Nilsson, S. Radel, S. Sadhal, M. Wiklund, Lab Chip **11**, 3579 (2011)
19. B.W. Drinkwater, Lab Chip **16**, 2360 (2016)
20. A. Scheeline, R.L. Behrens, Biophys. Chem. **165–166**, 1 (2012)
21. L. Rayleigh, Philos. Mag. **3**, 338 (1902)
22. L. Rayleigh, Philos. Mag. **10**, 364 (1905)
23. L.V. King, Proc. R. Soc. A Math. Phys. Eng. Sci. **147**, 212 (1934)
24. K. Yosioka, Y. Kawasima, Acustica **5**, 167 (1955)
25. L.P. Gor'kov, Solviet Phys. Dokl. **6**, 773 (1962)
26. C.P. Lee, T. G. Wang, J. Acoust. Soc. Am. **94**, 1099 (1993)
27. R.T. Beyer, J. Acoust. Soc. Am. **63**, 1025 (1978)
28. F.E. Borgnis, Rev. Mod. Phys. **25**, 653 (1953)
29. A.P. Sarvazyan, O.V. Rudenko, W.L. Nyborg, Ultrasound Med. Biol. **36**, 1379 (2010)
30. J. Friend, L.Y. Yeo, Rev. Mod. Phys. **83**, 647 (2011)
31. B. Chu, R.E. Apfel, J. Acoust. Soc. Am. **72**, 1673 (1982)
32. H. Bruus, Lab Chip **11**, 3742 (2011)
33. H. Bruus, Lab Chip **12**, 20 (2012)
34. H. Bruus, Lab Chip **12**, 1014 (2012)
35. E.H. Trinh, J.L. Robey, Phys. Fluids **6**, 3567 (1994)
36. K. Hasegawa, Y. Abe, A. Kaneko, Y. Yamamoto, K. Aoki, Microgravity Sci. Technol. **21**, S9 (2009)
37. K. Hasegawa, Y. Abe, A. Goda, Npj Microgravity **2**, 16004 (2016)
38. M.A.B. Andrade, T.S. Ramos, F.T.A. Okina, J.C. Adamowski, Rev. Sci. Instrum. **85**, 45125 (2014)
39. X. Zheng, R.E. Apfel, J. Acoust. Soc. Am. **97**, 2218 (1995)
40. G.T. Silva, H. Bruus, Phys. Rev. E - Stat. Nonlinear, Soft Matter Phys. **90**, 63007 (2014)
41. L.D. Landau, E.M. Lifshitz, *Fluid mechanics: Landau and Lifshitz: course of theoretical physics* (Pergamon, Oxford, 1987)
42. L.E. Kinsler, A.R. Frey, A.B. Coppens, J.V. Sanders, *Fundamentals of acoustics* (Wiley, New York, 1999)
43. B.R. Munson, D.F. Young, T.H. Okiishi, W.W. Huebsch, *Fundamentals of fluid mechanics*, 6th edn. (Wiley, Roboken, 2009)
44. H. Bruus, *Theoretical microfluidics* (Oxford University Press, New York, 2008)
45. T. Hasegawa, T. Kido, T. Iizuka, C. Matsuoka, J. Acoust. Soc. Japan **21**, 145 (2000)
46. P. Glynne-Jones, P.P. Mishra, R.J. Boltryk, M. Hill, J. Acoust. Soc. Am. **133**, 1885 (2013)
47. O. Manneberg, Multidimensional ultrasonic standing wave manipulation in microfluidic chips, Doctoral Thesis, Royal Institute of Technology, Stockholm, Sweden, 2009
48. D. Foresti, M. Nabavi, M. Klingauf, A. Ferrari, D. Poulikakos, Proc. Natl. Acad. Sci. **110**, 12549 (2013)
49. D. Foresti, D. Poulikakos, Phys. Rev. Lett. **112**, 1 (2014)
50. M.A.B. Andrade, F.C. Buiochi, J. Adamowski, IEEE Trans. Ultrason. Ferroelectr. Freq. Control **57**, 469 (2010)
51. M.A.B. Andrade, N. Perez, F. Buiochi, J.C. Adamowski, IEEE Trans. Ultrason. Ferroelectr. Freq. Control **58**, 1674 (2011)
52. M. Barmatz, P. Collas, Acoust. Soc. Am. **77**, 928 (1985)
53. A. Marzo, S.A. Seah, B.W. Drinkwater, D.R. Sahoo, B. Long, S. Subramanian, Nat. Commun. **6**, 8661 (2015)
54. M.A.B. Andrade, N. Pérez, J.C. Adamowski, Rev. Bras. Ensino Física **37**, 2304 (2015)
55. N. Perez, M.A.B. Andrade, R. Canetti, J.C. Adamowski, J. Appl. Phys. **116**, 184903 (2014)
56. E.H. Trinh, C.J. Hsu, J. Acoust. Soc. Am. **80**, 1757 (1986)
57. T. Hasegawa, K. Yosioka, J. Acoust. Soc. Am. **46**, 1139 (1969)
58. T. Hasegawa, J. Acoust. Soc. Am. **65**, 32 (1979)
59. P.L. Marston, J. Acoust. Soc. Am. **120**, 3518 (2006)
60. J. Wu, G. Du, J. Acoust. Soc. Am. **87**, 997 (1989)
61. P.L. Marston, J. Acoust. Soc. Am. **125**, 3539 (2009)
62. G. Barrios, R. Rechtman, J. Fluid Mech. **596**, 191 (2008)
63. D. Haydock, J. Phys. A Math. Gen. **38**, 3265 (2005)
64. F. Cai, L. Meng, C. Jiang, Y. Pan, H. Zheng, J. Acoust. Soc. Am. **128**, 1617 (2010)
65. D. Foresti, M. Nabavi, D. Poulikakos, J. Fluid Mech. **709**, 581 (2012)
66. J. Wang, J. Dual, J. Phys. A Math. Theor. **42**, 285502 (2009)
67. N. Bjelobrk, D. Foresti, M. Dorrestijn, M. Nabavi, D. Poulikakos, Appl. Phys. Lett. **97**, 161904 (2010)
68. Z.Y. Hong, W. Zhai, N. Yan, B. Wei, J. Acoust. Soc. Am. **135**, 2553 (2014)

69. D. Foresti, N. Bjelobrk, M. Nabavi, D. Poulikakos, J. Appl. Phys. **109**, 93503 (2011)
70. W.J. Xie, B. Wei, Appl. Phys. Lett. **79**, 881 (2001)
71. Y. Liu, J. Hu, C. Zhao, IEEE Trans. Ultrason. Ferroelectr. Freq. Control **57**, 1443 (2010)
72. P. Zhang, T. Li, J. Zhu, X. Zhu, S. Yang, Y. Wang, X. Yin, X. Zhang, Nat. Commun. **5**, 4316 (2014)
73. P. Collas, M. Barmatz, C. Shipley, J. Acoust. Soc. Am. **86**, 777 (1989)
74. T. Schwarz, P. Hahn, G. Petit-Pierre, J. Dual, Microfluid. Nanofluidics **18**, 65 (2014)
75. A. Kundt, Ann. Phys. **203**, 497 (1866)
76. K. Bücks, H. Müller, Zeitschrift Für Phys. **84**, 75 (1933)
77. H.W.S. Clair, Rev. Sci. Instrum. **12**, 250 (1941)
78. H.W.S. Clair, Ind. Eng. Chem. **41**, 2434 (1949)
79. C.H. Allen, I. Rudnick, J. Acoust. Soc. Am. **19**, 857 (1947)
80. T.G. Wang, M.M. Saffren, D.D. Elleman, "Acoustic Chamber for weightless positioning," in AIAA 12th Aerospace Sciences Meeting. 74–155 (1974)
81. R.R. Whymark, Ultrasonics **13**, 251 (1975)
82. W. Oran, L. Berge, H. Parker, Rev. Sci. Instrum. **51**, 626 (1980)
83. C.A. Rey, U.S. Patent 4,284,403 (1981)
84. E. Lierke, R. Grossbach, K. Flögel, P. Clancy, "Acoustic positioning for space processing of materials science samples in mirror furnaces," in IEEE Ultrason. Symp. (1983), pp. 1129–1139. https://doi.org/10.1109/ULTSYM.1983.198240
85. E.H. Trinh, Rev. Sci. Instrum. **56**, 2059 (1985)
86. P.M. Gammel, A.P. Croonquist, T.G. Wang, J. Acoust. Soc. Am. **83**, 496 (1988)
87. C.A. Rey, D.R. Merkley, G.R. Hammarlund, T.J. Danley, Metall. Trans. A. **19**, 2619 (1988)
88. T. Otsuka, K. Higuchi, K. Seya, Jpn. J. Appl. Phys. **29**, 170 (1990)
89. C. Zhuyou, L. Shuqin, L. Zhimin, G. Mingli, M. Yulong, W. Chenghao, Powder Technol. **69**, 125 (1992)
90. E.G. Lierke, Acustica **82**, 220 (1996)
91. C.R. Field, A. Scheeline, Rev. Sci. Instrum. **78**, 125102 (2007)
92. T.L. Stephens, R.S. Budwig, Rev. Sci. Instrum. **78**, 14901 (2007)
93. T. Kozuka, K. Yasui, T. Tuziuti, A. Towata, Y. Iida, Jpn. J. Appl. Phys. **47**, 4336 (2008)
94. J.K.R. Weber, C.A. Rey, J. Neuefeind, C.J. Benmore, Rev. Sci. Instrum. **80**, 83904 (2009)
95. Z.Y. Hong, W.J. Xie, B. Wei, Rev. Sci. Instrum. **82**, 74904 (2011)
96. V. Vandaele, A. Delchambre, P. Lambert, J. Appl. Phys. **109**, 124 (2011)
97. S. Baer, M.A.B. Andrade, C. Esen, J.C. Adamowski, G. Schweiger, A. Ostendorf, Rev. Sci. Instrum. **82**, 105111 (2011)
98. R.R. Boullosa, A. Pérez-López, R. Dorantes-Escamilla, J. Appl. Res. Technol. **11**, 857 (2013)
99. A. Stindt, M.A.B. Andrade, M. Albrecht, J.C. Adamowski, U. Panne, J. Riedel, Rev. Sci. Instrum. **85**, 15110 (2014)
100. M.A.B. Andrade, N. Pérez, J.C. Adamowski, Appl. Phys. Lett. **106**, 14101 (2015)
101. D. Zang, J. Li, Z. Chen, Z. Zhai, X. Geng, B.P. Binks, Langmuir **31**, 11502 (2015)
102. K. Melde, A.G. Mark, T. Qiu, P. Fischer, Nature **537**, 518 (2016)
103. M.H. Kandemir, M. Caliskan, J. Sound Vib. **382**, 227 (2016)
104. A. Marzo, A. Barnes, B.W. Drinkwater, Rev. Sci. Instrum. **88**, 85105 (2017)
105. J. C. Fletcher, T. G. Wang, M. M. Saffren, and D. D. Elleman, U.S. Patent 3,882,732 (1975)
106. T. Wang, E. Trinh, W. Rhim, D. Kerrisk, M. Barmatz, D. Elleman, Acta Astronaut. **11**, 233 (1984)
107. T. Wang, "Acoustic levitation and manipulation for space applications," in IEEE Ultrason. Symp. (1979), pp. 471–475. https://doi.org/10.1109/ULTSYM.1979.197246
108. M. B. Barmatz, U.S. Patent 4,393,706 (1983)
109. T.G. Wang, E.H. Trinh, A.P. Croonquist, D.D. Elleman, Phys. Rev. Lett. **56**, 452 (1986)
110. T.G. Wang, F.H. Busse, J. Acoust. Soc. Am. **69**, 1634 (1981)
111. E. Trinh, J. Robey, N. Jacobi, T. Wang, J. Acoust. Soc. Am. **79**, 604 (1986)
112. E.H. Trinh, C. Hsu, J. Acoust. Soc. Am. **79**, 1335 (1986)
113. T.G. Wang, A.V. Anilkumar, C.P. Lee, K.C. Lin, J. Fluid Mech. **276**, 389 (1994)
114. T.G. Wang, A.V. Anilkumar, C.P. Lee, J. Fluid Mech. **308**, 1 (1996)
115. E.G. Lierke, Acta Acust. United with Acust. **88**, 206 (2002)
116. E.G. Lierke, L. Holitzner, Acta Acust. United with Acust. **99**, 302 (2013)
117. J. Leiterer, F. Delißen, F. Emmerling, A.F. Thünemann, U. Panne, Anal. Bioanal. Chem. **391**, 1221 (2008)
118. J. Schenk, L. Tröbs, F. Emmerling, J. Kneipp, U. Panne, M. Albrecht, Anal. Methods **4**, 1252 (2012)
119. H. Hatano, Y. Kanai, Y. Ikegami, T. Fujii, K. Saito, Jpn. J. Appl. Phys. **21**, 202 (1982)
120. S.L. Min, R.G. Holt, R.E. Apfel, J. Acoust. Soc. Am. **91**, 3157 (1992)
121. D. Zang, K. Lin, L. Li, Z. Chen, X. Li, X. Geng, Appl. Phys. Lett. **110**, 121602 (2017)
122. W.J. Xie, C.D. Cao, Y.J. Lü, B. Wei, Phys. Rev. Lett. **89**, 104304 (2002)
123. X. Jiao, G. Liu, J. Liu, X. Liu, Proc. Inst. Mech. Eng. Part C-journal. Mech. Eng. Sci. **227**, 2504 (2013)
124. Z.Y. Hong, W.J. Xie, B. Wei, J. Appl. Phys. **107**, 14901 (2010)
125. D. Foresti, G. Sambatakakis, S. Bottan, D. Poulikakos, Sci. Rep. **3**, 3176 (2013)
126. Y. Hashimoto, Y. Koike, S. Ueha, J. Acoust. Soc. Japan **16**, 189 (1995)
127. Y. Hashimoto, Y. Koike, S. Ueha, J. Acoust. Soc. Am. **100**, 2057 (1996)
128. Y. Hashimoto, Y. Koike, S. Ueha, J. Acoust. Soc. Am. **103**, 3230 (1998)
129. T. Hatanaka, Y. Koike, K. Nakamura, S. Ueha, Y. Hashimoto, Japanese J. Appl. Physics, Part 2 Lett. **38**, L1284 (1999)
130. E. Matsuo, Y. Koike, K. Nakamura, S. Ueha, Y. Hashimoto, Ultrasonics **38**, 60 (2000)
131. S. Ueha, Y. Hashimoto, Y. Koike, Ultrasonics **38**, 26 (2000)
132. G. Reinhart, J. Hoeppner, J. Zimmermann, "Non-contact wafer handling using high-intensity ultrasonics," in 2001 IEEE/SEMI Adv. Semicond. Manuf. Conf. (2001), pp. 139–140. https://doi.org/10.1109/ASMC.2001.925636
133. H. Nomura, T. Kamakura, K. Matsuda, J. Acoust. Soc. Am. **111**, 1578 (2002)
134. A. Minikes, I. Bucher, S. Haber, J. Acoust. Soc. Am. **116**, 217 (2004)
135. T. Ide, J.R. Friend, K. Nakamura, S. Ueha, Jpn. J. Appl. Phys. **44**, 4662 (2005)
136. J. Li, P. Liu, H. Ding, W. Cao, Sensors Actuators A Phys. **171**, 260 (2011)
137. Z.Y. Hong, P. Lü, D.L. Geng, W. Zhai, N. Yan, B. Wei, Rev. Sci. Instrum. **85**, 104904 (2014)
138. C. Chen, J. Wang, B. Jia, F. Li, J. Intell. Mater. Syst. Struct. **25**, 755 (2014)
139. S. Zhao, S. Mojrzisch, J. Wallaschek, Mech. Syst. Signal Process. **36**, 168 (2013)
140. T. Ide, J. Friend, K. Nakamura, S. Ueha, Sensors Actuators A Phys. **135**, 740 (2007)
141. T. Watanabe, S. Fukui, Proc. - IEEE Int. Conf. Robot. Autom. **1**, 1134 (1995)
142. M. Wiertlewski, R. Fenton Friesen, J.E. Colgate, Proc. Natl. Acad. Sci. **113**, 9210 (2016)

143. M. Biet, F. Giraud, B. Lemaire-Semail, IEEE Trans. Ultrason. Ferroelectr. Freq. Control **54**, 2678 (2007)
144. T. Sednaoui, E. Vezzoli, B. Dzidek, B. Lemaire-Semail, C. Chappaz, M. Adams, "Experimental evaluation of friction reduction in ultrasonic devices," in IEEE World Haptics Conf. WHC 2015 (2015), pp. 37–42. https://doi.org/10.1109/WHC.2015.7177688
145. S. Ueha, Rev. Acústica **33**, 21 (2002)
146. M. Takasaki, D. Terada, Y. Kato, Y. Ishino, T. Mizuno, Phys. Procedia **3**, 1059 (2010)
147. S. Chino, Y. Kato, Y. Ishino, M. Takasaki, T. Mizuno, "Actuation force characteristics of ultrasonic suspension for minute object," in IEEE Int. Ultrason. Symp. IUS (2011), pp. 1218–1221. https://doi.org/10.1109/ULTSYM.2011.0300
148. M. Takasaki, S. Chino, Y. Kato, Y. Ishino, T. Mizuno, Key Eng. Mater. **523–524**, 727 (2012)
149. K. Uchiage, Y. Ishino, M. Takasaki, T. Mizuno, "Enlargement of floator size in ultrasonic suspension by arranging the shape of vibrating surface," in IEEE Int. Ultrason. Symp. IUS (2014), pp. 2510–2513. https://doi.org/10.1109/ULTSYM.2014.0626
150. S. Zhao, J. Wallaschek, Arch. Appl. Mech. **81**, 123 (2011)
151. M.A.B. Andrade, F.T.A. Okina, A.L. Bernassau, J.C. Adamowski, J. Acoust. Soc. Am. **141**, 4148 (2017)
152. J. Lee, S.Y. Teh, A. Lee, H.H. Kim, C. Lee, K.K. Shung, Appl. Phys. Lett. **95**, 73701 (2009)
153. D. Baresch, J.L. Thomas, R. Marchiano, Phys. Rev. Lett. **116**, 24301 (2016)
154. A. Marzo, A. Ghobrial, L. Cox, M. Caleap, A. Croxford, B.W. Drinkwater, Appl. Phys. Lett. **110**, 14102 (2017)
155. G. Memoli, M. Caleap, M. Asakawa, D.R. Sahoo, B.W. Drinkwater, S. Subramanian, Nat. Commun. **8**, 14608 (2017)
156. T.G. Wang, H. Kanber, I. Rudnick, Phys. Rev. Lett. **38**, 128 (1977)
157. A. Haake, J. Dual, Ultrasonics **40**, 317 (2002)
158. C.R.P. Courtney, C.-K. Ong, B.W. Drinkwater, A.L. Bernassau, P.D. Wilcox, D.R.S. Cumming, Proc. R. Soc. A Math. Phys. Eng. Sci. **468**, 337 (2012)
159. A. Grinenko, C.K. Ong, C.R.P. Courtney, P.D. Wilcox, B.W. Drinkwater, Appl. Phys. Lett. **101**, 233501 (2012)
160. T. Matsui, E. Ohdaira, N. Masuzawa, M. Ide, Jpn. J. Appl. Phys. **34**, 2771 (1995)
161. T. Kozuka, K. Yasui, T. Tuziuti, A. Towata, Y. Iida, Jpn. J. Appl. Phys. **46**, 4948 (2007)
162. D. Koyama, K. Nakamura, IEEE Trans. Ultrason. Ferroelectr. Freq. Control **57**, 1152 (2010)
163. D. Koyama, K. Nakamura, IEEE Trans. Ultrason. Ferroelectr. Freq. Control **57**, 1434 (2010)
164. Y. Ito, D. Koyama, K. Nakamura, Acoust. Sci. Technol. **31**, 420 (2010)
165. G. Thomas, M.A. Andrade, J. Adamowski, E. Silva, IEEE Trans. Ultrason. Ferroelectr. Freq. Control **64**, 839 (2017)
166. R. Kashima, D. Koyama, M. Matsukawa, IEEE Trans. Ultrason. Ferroelectr. Freq. Control **62**, 2161 (2015)
167. N. Bjelobrk, M. Nabavi, D. Poulikakos, J. Appl. Phys. **112**, 53510 (2012)
168. Y. Ochiai, T. Hoshi, J. Rekimoto, PLoS One **9**, e97590 (2014)
169. T. Hoshi, Y. Ochiai, J. Rekimoto, Jpn. J. Appl. Phys. **53**, 07KE07 (2014)
170. Y. Ochiai, T. Hoshi, and J. Rekimoto, ACM Trans. Graph. **33**, Article 85 (2014)
171. T. Omirou, A. Marzo, S.A. Seah, S. Subramanian, "LeviPath: Modular Acoustic Levitation for 3D Path Visualisations," in Proc. 33rd Annu. ACM Conf. Hum. Factors Comput. Syst. (2015), pp. 309–312. https://doi.org/10.1145/2702123.2702333
172. C.T. Vi, A. Marzo, D. Ablart, G. Memoli, S. Subramanian, B. Drinkwater, M. Obrist, "TastyFloats : A Contactless Food Delivery System," in Proc. 2017 ACM Int. Conf. Interact. Surfaces Spaces (2017), pp. 161–170. https://doi.org/10.1145/3132272.3134123
173. D. Koyama, K. Nakamura, S. Ueha, IEEE Trans. Ultrason. Ferroelectr. Freq. Control **54**, 2337 (2007)
174. D. Koyama, H. Takei, K. Nakamura, S. Ueha, IEEE Trans. Ultrason. Ferroelectr. Freq. Control **55**, 1823 (2008)
175. D. Koyama, K. Nakamura, Jpn. J. Appl. Phys. **48**, 07GM07 (2009)
176. K. Chen, S. Gao, Y. Pan, P. Guo, Appl. Phys. Lett. **109**, 123503 (2016)